doi:10.1016/j.jmb.2004.04.010 J. Mol. Biol. (2004) 339, 751–771

JMB

Available online at www.sciencedirect.com

SCIENCE DIRECT®

ELSEVIER

Effects of Temperature and ATP on the Kinetic Mechanism and Kinetic Step-size for *E. coli* RecBCD Helicase-catalyzed DNA Unwinding

Aaron L. Lucius and Timothy M. Lohman*

Department of Biochemistry and Molecular Biophysics Washington University School of Medicine, 660 S. Euclid Ave. Box 8231, St. Louis, MO 63110-1093, USA

The kinetic mechanism by which *Escherichia coli* RecBCD helicase unwinds duplex DNA was studied using a fluorescence stopped-flow method. Single turnover DNA unwinding experiments were performed using a series of fluorescently labeled DNA substrates containing duplex DNA regions ranging from 24 bp to 60 bp. All or no DNA unwinding time courses were obtained by monitoring the changes in fluorescence resonance energy transfer between a Cy3 donor and Cy5 acceptor fluorescent pair placed on opposite sides of a nick in the duplex DNA. From these experiments one can determine the average rates of DNA unwinding as well as a kinetic step-size, defined as the average number of base-pairs unwound between two successive rate-limiting steps repeated during DNA unwinding. In order to probe how the kinetic step-size might relate to a mechanical step-size, we performed single turnover experiments as a function of [ATP] and temperature. The apparent unwinding rate constant, k_{Uapp}, decreases with decreasing [ATP], exhibiting a hyperbolic dependence on [ATP] ($K_{1/2} = 176(\pm 30)$ μM) and a maximum rate of $k_{Uapp} = 204(\pm 4)$ steps s^{-1} ($mk_{Uapp} = 709(\pm 14)$ bp s^{-1}) (10 mM $MgCl_2$, 30 mM NaCl (pH 7.0), 5% (v/v) glycerol, 25.0 °C). k_{Uapp} also increases with increasing temperature (10–25 °C), with $E_a = 19(\pm 1)$ kcal mol^{-1}. However, the average kinetic step-size, $m = 3.9(\pm 0.5)$ bp $step^{-1}$, remains independent of [ATP] and temperature. This indicates that even though the values of the rate constants change, the same elementary kinetic step in the unwinding cycle remains rate-limiting over this range of conditions and this kinetic step remains coupled to ATP binding. The implications of the constancy of the measured kinetic step-size for the mechanism of RecBCD-catalyzed DNA unwinding are discussed.

*Corresponding author

Keywords: motor; helicase; FRET; recombination; ATPase

Introduction

The *Escherichia coli* RecBCD enzyme, a heterotrimer of the RecB (134 kDa), RecC (129 kDa) and RecD (67 kDa) proteins,[1–3] is essential for genetic recombination and has double-stranded (ds) and single-stranded (ss) DNA exonuclease, ssDNA endonuclease, DNA-dependent ATPase, and helicase activities.[4,5] Both the RecB and RecD polypeptides are members of the SF1 helicase superfamily,[6] and both isolated proteins have helicase activity, with RecB having 3′ to 5′ polarity,[7] while RecD has 5′ to 3′ polarity.[8] Hence, it has been proposed that the RecBCD holoenzyme is a bipolar DNA helicase, with two motors that move with opposite polarities along each single strand of the DNA,[8,9] and thus in the same net direction along the duplex.

A variety of evidence indicates that RecBCD initiates unwinding of duplex DNA at a dsDNA end.[10] Genetic results indicate that an important intracellular substrate for RecBCD is linear dsDNA,[11] and the helicase activity of the purified enzyme has a strong preference for linear dsDNA

Present address: A. L. Lucius, Department of Human Biological Chemistry and Genetics, The University of Texas Medical Branch at Galveston, Room 5.120 Medical Research Building, Galveston, TX 77555-1053, USA.

Abbreviations used: bp, base-pairs; dsDNA, double-stranded DNA; ssDNA, single-stranded DNA; NLLS, non-linear least-squares; βME, β-mercaptoethanol.

E-mail address of the corresponding author: lohman@biochem.wustl.edu

with blunt or nearly blunt ends.[12,13] Analysis of partially unwound DNA by electron microscopy showed that the enzyme initiates unwinding at the end of dsDNA and can unwind >20,000 bp of DNA with high processivity at rates of ~350 bp s^{-1}.[14] Depending on solution conditions, the rate of unwinding can approach 500 bp s^{-1} at 25 °C and 1000 bp s^{-1} at 37 °C with sufficient processivity to unwind DNA with an average length of 30,000 bp.[15–17] In the absence of ATP, which is required for processive DNA unwinding, the enzyme binds with high affinity to a dsDNA end, most tightly to ends possessing short ssDNA extensions.[12,18] In this complex the RecB polypeptide can be crosslinked by UV-irradiation to the 3′ DNA strand, whereas the RecC and RecD polypeptides can be crosslinked to the 5′ DNA strand.[19] Binding of RecBCD to the duplex end results in a perturbation of the conformation, possibly melting, of ~5–6 bp in a Mg^{2+}-dependent, but ATP-independent, reaction as determined from chemical protection experiments[20] using $KMnO_4$.

We have examined the RecBCD-catalyzed DNA unwinding mechanism using single turnover chemical quenched-flow kinetic techniques.[21] From that study we determined that RecBCD unwinds with an average "kinetic step-size", $m = 3.9(\pm 1.3)$ bp $step^{-1}$, and an average unwinding rate constant of $k_U = 196(\pm 77)$ steps s^{-1} ($mk_U = 790(\pm 23)$ bp s^{-1}) at 25.0 °C (5 mM ATP, 10 mM $MgCl_2$, 30 mM NaCl (pH 7.0), 5% (v/v) glycerol). The kinetic step-size determined in those experiments is defined as the average number of base-pairs unwound between two successive rate-limiting steps that are repeated during DNA unwinding. In the preceding manuscript, we describe a fluorescence stopped-flow method to examine RecBCD-catalyzed DNA unwinding yielding time-courses with increased precision and that require significantly shorter acquisition times.[38] Using that method we re-examined RecBCD-catalyzed DNA unwinding under the same solution conditions and estimated an average kinetic "step-size", $m = 3.4(\pm 0.6)$ bp $step^{-1}$, and an average unwinding rate constant, $k_U = 200(\pm 40)$ steps s^{-1}.

Molecular motors, such as DNA helicases that must translocate along a DNA filament, can also be characterized by a mechanical step-size that represents the average distance moved by the center of mass of the enzyme per catalytic step (e.g. per ATP hydrolyzed). However, it is possible that the mechanical step-size could differ from the kinetic step-size, as defined here. In fact, if all domains within the enzyme do not move in unison or to the same extent, there could potentially be more than one mechanical step-size for a single enzyme. This seems even more likely for a DNA helicase such as RecBCD that possesses two ATPase sites and two helicase subunits (RecB and RecD). As an example, Bianco & Kowalczykowski[17] have proposed a "quantum inch worm model" for *E. coli* RecBC unwinding and translocation to explain their observation that the RecBC helicase appears able to bypass flexible ssDNA gaps in duplex DNA as large as ~23 nt. In this model, it was proposed that the enzyme has two DNA binding sites and that DNA unwinding by the rear binding site occurs in a series of small steps of a few bp, whereas the lead-binding site makes larger translocation steps of ~23 bp.[17] Therefore, in this model, the unwinding step-size would be smaller than the translocation or mechanical step-size.

Since there are many elementary kinetic steps that must be coupled to the movement of the enzyme (e.g. ATP binding, hydrolysis, product release, protein conformational changes and the unwinding of m bp), it is important to consider the relationship between a kinetic step-size and a mechanical step-size. If there is only one rate-limiting kinetic step that is repeated per mechanical step, then the kinetic step-size should equal the mechanical step-size. On the other hand, if two (or more) different kinetic steps with fortuitously similar rates occur per mechanical step, then the kinetic step-size would reflect only the average number of base-pairs unwound between these two (or more) different kinetic steps and thus can be smaller than the mechanical step-size. If this is the case, it is also possible that the measured kinetic step-size could change with solution conditions if the elementary rate-limiting step within the unwinding cycle also changes.[22] As such, it is important to determine if a single rate-limiting step is repeated per unwinding cycle or if multiple steps with similar rate constants occur during each cycle. In order to further probe the meaning of the kinetic step-size measured for RecBCD-catalyzed DNA unwinding, we have examined whether the measured kinetic step-size is dependent upon solution conditions ([ATP] and temperature).

Theoretical Background

Simulations of the effects of [ATP] on the measured kinetic parameters and the kinetic step-size for DNA unwinding

In order for a helicase to unwind DNA processively, repeated cycles of ATP binding, hydrolysis and product release must be coupled to the melting of some number of base-pairs, and mechanical movement (translocation) of the enzyme along the DNA filament. As discussed,[21,22] the single turnover DNA unwinding assays used in the experiments reported here are generally sensitive to the slowest steps that are repeated in the unwinding cycle. For example, in Scheme 1 a repeated rate-limiting step, designated k_U, might correspond to

$$HD \xrightarrow{k_U} I_1 \xrightarrow{k_U} I_2 \xrightarrow{k_U} \ldots \xrightarrow{k_U} I_{n-1} \xrightarrow{k_U} ssDNA$$

Scheme 1.

$$HD_L + ATP \underset{k_2}{\overset{k_1}{\rightleftharpoons}} HD_L \cdot ATP \xrightarrow{k_3} I_1 + ATP \underset{k_2}{\overset{k_1}{\rightleftharpoons}} I_1 \cdot ATP \xrightarrow{k_3} I_2 + ATP \ldots \xrightarrow{k_3} ssDNA$$

Scheme 2.

the actual unwinding step, but could also reflect any other step in the cycle (e.g. ADP or P_i release or a protein conformational change). If this repeated rate-limiting step occurs only once per mechanical step, then the kinetic step-size will equal the mechanical step-size.[22] However, if there are multiple kinetic steps per mechanical step and two or more of these steps have rate constants similar in magnitude to the rate-limiting step, then the kinetic step-size will be smaller than the mechanical step-size.

In order to demonstrate how changes in [ATP] could influence both the apparent kinetic parameters as well as the apparent kinetic step-size for DNA unwinding, we performed a series of simulations using Scheme 2. Each repeated unwinding cycle in Scheme 2 includes explicit steps for reversible ATP binding, followed by a step with rate constant k_3. The step with rate constant k_3 could be a conformational change or ATP hydrolysis, but we assume that all other steps in the cycle are fast relative to k_3. We simulated time-courses for DNA unwinding of a series of DNA molecules varying in duplex length as a function of ATP concentration with varying values for k_1, k_2, k_3, but a constant value of the kinetic step-size, $m = 4$ bp step^{-1}, under two sets of limiting conditions. The first condition assumes that ATP binding does not occur as a rapid equilibrium step (i.e. $k_3 \gg k_2$), whereas the second condition considers ATP binding to occur in a rapid equilibrium (i.e. $k_2 \gg k_3$). Non-linear least-squares (NLLS) analysis was then performed on the time-courses simulated at each ATP concentration using Scheme 1 to obtain estimates of the apparent unwinding rate, k_{Uapp}, and the apparent kinetic step-size, m_{app}.

ATP-binding step is not in rapid equilibrium ($k_2 \ll k_3$)

To examine the behavior of the apparent unwinding rate constant, k_{Uapp}, and the kinetic step-size, m_{app}, under conditions where the ATP-binding step is not in a rapid equilibrium, time-courses were simulated using Scheme 2 (equation (A3)) for [ATP] ranging from 10 nM to 5 mM, and the following parameters: $k_1 = 1 \times 10^8$ M^{-1} s^{-1}, $k_2 = 1$ s^{-1}, $k_3 = 50$ s^{-1}, $m = 4$ bp step^{-1} ($n = L/m$), for duplex lengths, $L = 24$, 30, 40, 48, and 60 bp. Here, the number of steps, n, represents the number of repetitions of the unwinding cycle, which consists of both the ATP-binding step and the step with rate constant k_3. For all simulations, the [ATP] was in excess over the [RecBCD] and thus the pseudo first-order rate constant, k_1[ATP], was used for the calculations (see Appendix A).

Figure 1 shows the dependence of k_{Uapp} and m_{app} on [ATP] obtained from NLLS analysis of the time-courses simulated using Scheme 2, but analyzed using Scheme 1 (equation (A2)). Figure 1a shows that at saturating [ATP], the value of k_{Uapp} is approximately constant at 50 s^{-1} down to 10 μM ATP, where a slight increase is observed. However,

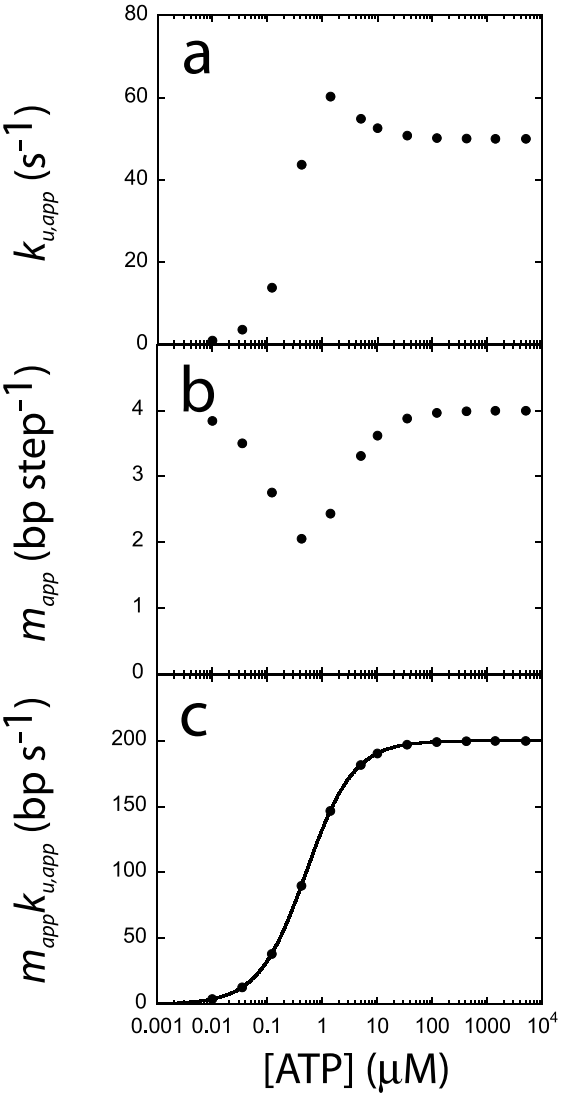

Figure 1. Dependence on ATP concentration of kinetic parameters obtained from global NLLS analysis of simulated DNA unwinding time-courses generated when a rapid equilibrium does not apply to the ATP-binding step. Time-courses were generated using Scheme 2 with: $k_1 = 1 \times 10^8$ M^{-1} s^{-1}, $k_2 = 1$ s^{-1}, $k_3 = 50$ s^{-1}, $n = L/m$, $m = 4$ bp step^{-1}, for duplex lengths of $L = 24$, 30, 40, 48, and 60 bp. Global NLLS analysis of these simulated time-courses was then performed using Scheme 1 and the resulting best-fit kinetic parameters were determined. a, Plot of k_{Uapp} *versus* ATP concentration exhibits a transition due to a change in the rate-limiting step from k_3 at high [ATP] to k_1[ATP] at low [ATP]. b, Dependence of the apparent kinetic step-size, m_{app} on [ATP]. c, Dependence of $m_{app}k_{Uapp}$ on [ATP]. The continuous line is a simulation using equation (5) and the best NLLS parameters: $(m_{app}k_{Uapp})_{max} = 200$ bp s^{-1} and $K_d = 500$ nM.

at ~1 μM ATP, k_{Uapp} exhibits a precipitous decrease with decreasing [ATP]. Figure 1b shows that m_{app} also depends on [ATP]. At excess [ATP], $m_{app} = 4$ bp step^{-1}, since only a single rate-limiting step is repeated in each cycle. However, as the [ATP] is decreased, m_{app} decreases until it reaches a value of 2 bp step^{-1}, corresponding to where $k_3 = k_1$[ATP]. Upon lowering the [ATP] further, m_{app} increases until it returns to a value of 4 bp step^{-1}. The reason for these effects is that at excess [ATP] the step with rate constant k_3 is rate-limiting and thus the time-courses are sensitive to only k_3, whereas as the [ATP] is lowered to an intermediate range, the time-courses become sensitive to both k_3 and k_1[ATP]. Finally, at very low [ATP] where ATP binding becomes completely rate-limiting, the time-courses are sensitive to only k_1[ATP]. Thus, the time-courses are again sensitive to only a single rate-limiting step (now ATP binding) and thus the value of m_{app} again approaches the actual value of 4 bp step^{-1}.

Finally, Figure 1c shows that the product, $m_{app}k_{Uapp}$, exhibits a hyperbolic dependence on [ATP]. A fit of these data to a hyperbolic function (equation (5)) predicts a maximum unwinding rate at saturating [ATP] of $k_{max} = (m_{app}k_{Uapp})_{max} = 200$ bp s^{-1} and a midpoint corresponding to a $K_{d,app} = 500$ nM, whereas the actual value of K_d for ATP binding used in the simulations was $K_d = k_2/k_1 = 10$ nM. Therefore, under these conditions, the midpoint does not provide an accurate estimate of the affinity for ATP binding, because equation (5) is valid only under rapid equilibrium conditions.[23]

ATP-binding step is in rapid equilibrium ($k_2 \gg k_3$)

To examine the behavior of k_{Uapp}, and the apparent kinetic step-size, m_{app}, under conditions where the ATP-binding step is in rapid equilibrium ($k_2 \gg k_3$), we simulated time-courses using Scheme 2 (equation (A3)) and the following parameters: $k_1 = 1 \times 10^8$ M^{-1} s^{-1}, $k_2 = 2 \times 10^4$ s^{-1}, $k_3 = 50$ s^{-1}, $m = 4$ bp step^{-1} ($n = L/m$), for $L = 24$, 30, 40, 48, and 60 bp and an [ATP] ranging from 10 μM to 5 mM. For these simulations, the equilibrium constant, $K_a = k_1/k_2 = 5 \times 10^3$ M^{-1} ($K_d = 200$ μM). The simulated time-courses were then fit to Scheme 1 (equation (A2)) as described above, to obtain the estimates of k_{Uapp}, and m_{app} plotted in Figure 2.

As shown in Figure 2a and b, both k_{Uapp} and $m_{app}k_{Uapp}$ exhibit hyperbolic dependences on [ATP]. NLLS fitting of the data in Figure 2a and b using equation (5) yields a maximum rate constant at saturating [ATP] of $k_{Uapp,max} = 50$ s^{-1}, $(m_{app}k_{Uapp})_{max} = 200$ bp s^{-1}, and $K_d = 200$ μM for both fits. These values are consistent with the parameters used to simulate the curves using Scheme 2 ($k_3 = 50$ s^{-1} and $K_d = k_2/k_1 = 200$ μM). In addition, Figure 2c shows that m_{app} remains constant at the input value of $m = 4$ bp step^{-1}, independent of [ATP]. This results from the fact that the same repeated step (k_3 in Scheme 2) remains rate limiting at all [ATP]. That is, under rapid equilibrium conditions, the rate of ATP binding is always much faster than k_3, although ATP binding is still linked to k_3. Therefore, although the simulated time-courses include two repeating

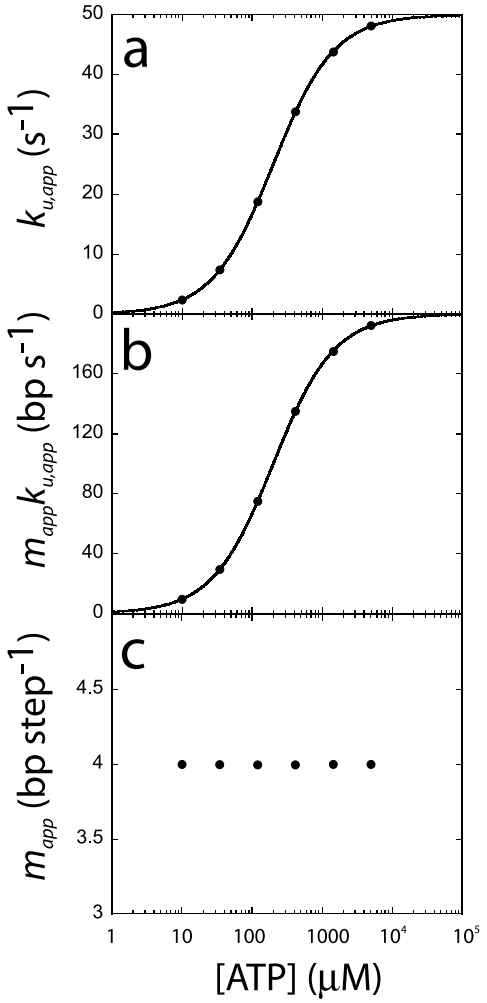

Figure 2. Dependence on ATP concentration of kinetic parameters obtained from global NLLS analysis of simulated DNA unwinding time-courses generated when a rapid equilibrium applies to the ATP-binding step. To simulate rapid equilibrium conditions ($k_2 \gg k_3$) time-courses were simulated using Scheme 2 and the following parameters: $k_1 = 1 \times 10^8$ M^{-1} s^{-1}, $k_2 = 2 \times 10^4$ s^{-1}, $k_3 = 50$ s^{-1}, $n = L/m$, $m = 4$ bp step^{-1}, for duplex lengths of $L = 24$, 30, 40, 48, and 60 bp. Hence, the equilibrium constant for ATP binding is $K_d = k_2/k_1 = 200$ μM. Global NLLS analysis of the simulated time courses was then performed using Scheme 1 and the resulting best-fit kinetic parameters were determined. a, Hyperbolic dependence of k_{Uapp} on [ATP]. The continuous line is a simulation using equation (5) and the best NLLS parameters: $k_{Umax} = 50$ s^{-1}, and $K_d = 200$ μM. b, Hyperbolic dependence of $m_{app}k_{Uapp}$ on [ATP]. The continuous line is a simulation using equation (5) and the best NLLS parameters: $(m_{app}k_{Uapp})_{max} = 200$ bp s^{-1}, and $K_d = 200$ μM. c, The apparent kinetic step-size, m_{app}, is independent of ATP concentration.

steps per cycle, one of those repeated steps (k_3 in Scheme 2) always remains the rate-limiting step at all [ATP] as long as the ATP-binding step occurs as a rapid equilibrium.

Scheme 2 specifies that one ATP-binding event is coupled to the unwinding of m bp in each unwinding cycle. An alternative scenario is that one ATP-binding event is coupled to the unwinding of each base-pair, with rate constant, k_U, and that a succession of m bp are unwound rapidly, followed by a rate-limiting step, k_3, that is also coupled to an ATP-binding event. Such a scenario is depicted in Scheme 3, which, as written, describes a single cycle for unwinding of m bp. This cycle would be repeated L/m times, where L is the length of the duplex to be unwound. If $k_U \gg k_3$ in Scheme 3 and all ATP-binding steps are in rapid equilibrium, then the cycle in Scheme 3 reduces to the cycle in Scheme 2 in which a single ATP-binding step is coupled to the step with rate constant k_3, with m bp unwound per $m + 1$ ATP. Therefore, in this limit, m_{app} will be independent of [ATP] as shown in Figure 2c. These results indicate that if the apparent kinetic step-size is independent of [ATP] one can conclude that there is at least one ATP-binding step within the cycle, but one cannot conclude anything about the stoichiometry of ATP required to unwind those m bp. The only way to differentiate Scheme 2 from Scheme 3, experimentally, is to have an independent measure of the stoichiometry of ATP hydrolyzed per kinetic step-size.

Results

Effect of [ATP] on RecBCD-catalyzed DNA unwinding

In our previous studies of RecBCD-catalyzed DNA unwinding we determined an apparent kinetic step-size of $m_{app} = 3.9(\pm 1.3)$ bp step^{-1} using chemical quenched-flow techniques[21] and $m_{app} = 3.4(\pm 0.6)$ bp step^{-1} using stopped-flow fluorescence methods,[38] under the same solution conditions (5 mM ATP, 10 mM $MgCl_2$, 30 mM NaCl (pH 7.0), 5% glycerol, 25.0 °C). Here, we examine the effect of [ATP] on the kinetic parameters for DNA unwinding and m_{app} to determine if the same kinetic step that is repeated in the cycle remains rate limiting at all [ATP]. As discussed above, these results will bear on the interpretation of m_{app} and its relationship to a mechanical step-size. These experiments will also provide a further test of our previous conclusion that additional kinetic steps with rate constant k_C occur within the mechanism (preceding unwinding), but are not involved directly in DNA unwinding (see Scheme 5).[21,38] If the steps with rate constant k_C are not involved directly in the DNA unwinding cycle, then both the rate constant (k_C) and the number of times it occurs (h) should be independent of [ATP].

The time-courses for RecBCD-catalyzed DNA unwinding were examined by monitoring the increase in Cy3 fluorescence upon addition of ATP to a pre-equilibrated solution containing RecBCD pre-bound to a series of Cy3/Cy5-labeled DNA substrates as described.[38] Single turnover experiments were performed at a series of [ATP] (final [ATP] = 5 mM, 1.4 mM, 416, 120, 75, 37.5, and 10 μM) by including heparin in the ATP solution. The heparin serves as a trap for any free RecBCD enzyme, thus ensuring that the experiments are single turnover (single round) with respect to DNA unwinding. At each [ATP], a series of DNA substrates varying in duplex DNA length ($L = 24$, 29, 37, 40, 43, 48, 53, and 60 bp) were unwound and the resulting time courses are shown in Figure 3, which shows that as the [ATP] is decreased, the qualitative shapes of the time-courses remain unchanged, although the macroscopic rate of RecBCD-catalyzed DNA unwinding decreases, consistent with previous studies.[16] For all time-courses at each [ATP], a lag period is observed in the time-course for the formation of fully unwound DNA. This is expected for an "all or none" assay such as this, if RecBCD unwinds the DNA in a series of repeated steps, where the value of the rate constant is similar for each repeated step.[22]

For each [ATP], we first performed a global NLLS analysis of the set of time-courses determined for the series of duplex lengths, L, using the simplified Scheme 4 (equation (1)) to obtain the relationship between the observed number of steps, n_{obs}, and L. For each global NLLS fitting at a given [ATP], the parameters k_U, and k_{NP} were constrained to be identical for all duplex lengths, while the amplitude, A_1, the observed number of steps, n_{obs}, and the fraction of productively bound complexes, x were allowed to float for each duplex length. Figure 4 shows plots of n_{obs} *versus* L determined at each [ATP]. In each case, n_{obs} exhibits a linear dependence on L; however, a positive intercept is observed for the data determined at the five highest [ATP] (5 mM, 1.4 mM, 416, 120, and 75 μM), whereas the linear dependence intersects with the origin at the two lowest [ATP] (37.5 μM and 10 μM).

As discussed,[21,22] a plot of n_{obs} *versus* duplex DNA length, L, can display a positive y-intercept if the mechanism describing the time-courses contains additional kinetic steps that are not part of the repeated cycles of DNA unwinding.[38] Therefore, the data in Figure 4 indicate that additional

$$HD_L \underset{k_2}{\overset{k_1[T]}{\rightleftharpoons}} HD_L \cdot T \xrightarrow{k_U} I_{L-1} \underset{k_2}{\overset{k_1[T]}{\rightleftharpoons}} I_{L-1} \cdot T \xrightarrow{k_U} I_{L-2} \ldots I_{L-m} \underset{k_2}{\overset{k_1[T]}{\rightleftharpoons}} I_{L-m} \cdot T \xrightarrow{k_3} I^*_{L-m}$$

Scheme 3.

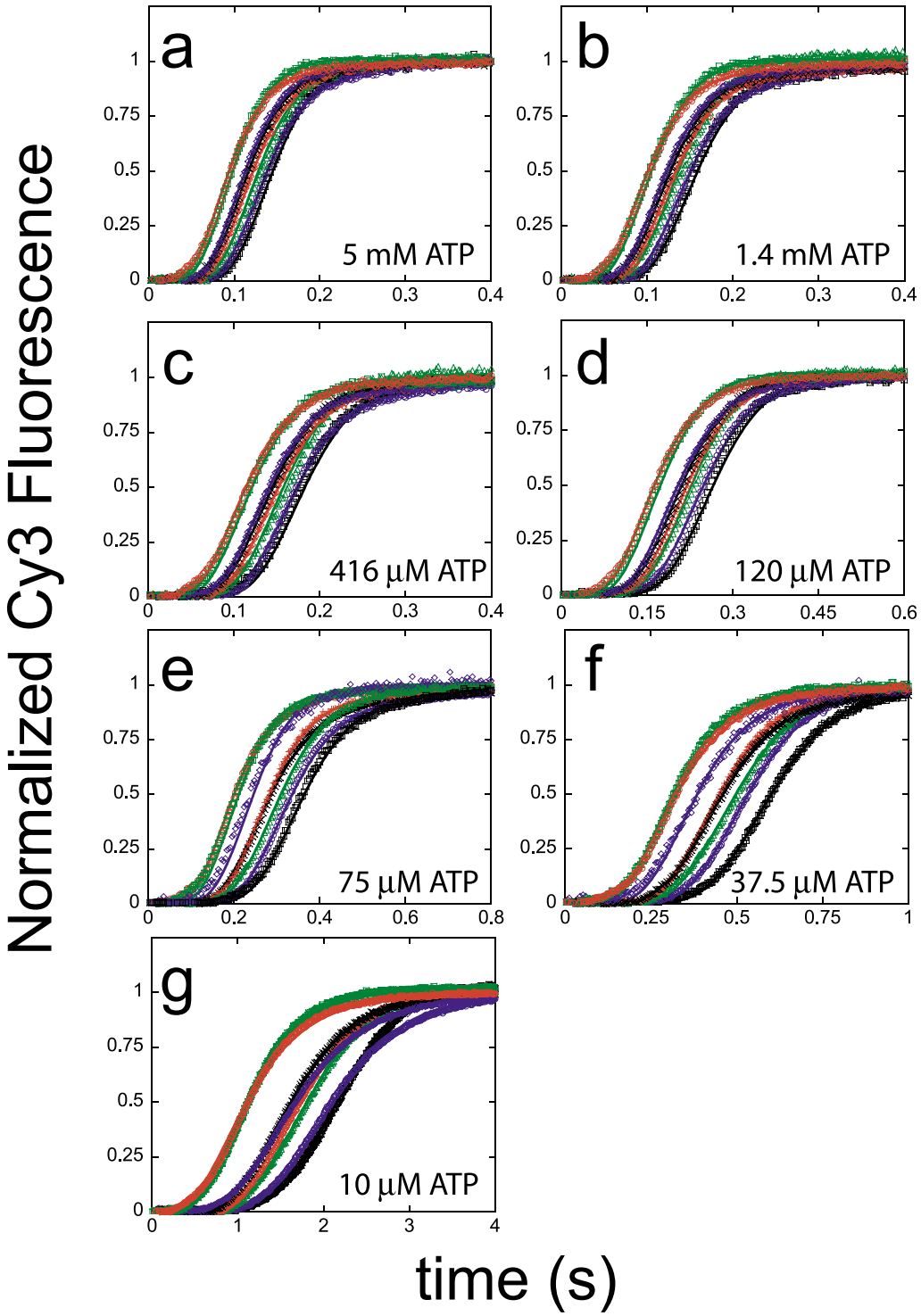

Figure 3. Effect of [ATP] on single turnover RecBCD-catalyzed DNA unwinding time courses. Stopped-flow kinetics experiments monitoring changes in Cy3 fluorescence of labeled DNA substrates were performed by pre-incubating 200 nM RecBCD with 40 nM DNA substrate in Buffer M at 25 °C. Reactions were initiated by rapidly mixing the RecBCD–DNA solution with a solution containing ATP (final [ATP] noted in each panel) and heparin (1.6 mg ml^{-1} final concentration) in buffer M. The Cy3 fluorophore was excited at $\lambda_{ex} = 515$ nm, and the Cy3 fluorescence was monitored at 570 nm using an interference filter. For each panel the duplex lengths used are: $L = 24$ bp (○), $L = 29$ bp (□), $L = 37$ bp (◇), $L = 40$ bp (×), $L = 43$ bp (+), $L = 48$ bp (△), $L = 53$ bp (○), and $L = 60$ bp (□). The smooth curves overlaying each time-course are simulations using Scheme 5 (equation (3)) and the best-fit parameters given in Table 1.

$$\begin{array}{l}(R \bullet D)_{NP} \\ \downarrow k_{NP} \\ (R \bullet D)_{L} \xrightarrow{k_U} I_{(L-m)} \xrightarrow{k_U} ....I_{(L-im)}... \xrightarrow{k_U} ssDNA\end{array}$$

Scheme 4.

steps, not involved in the repeated cycles of DNA unwinding, are needed to describe these time-courses.[21,22] However, the time-courses obtained at the two lower [ATP] suggest either that these time-courses are not sensitive to the presence of these additional steps or that these steps no longer occur in the mechanism.

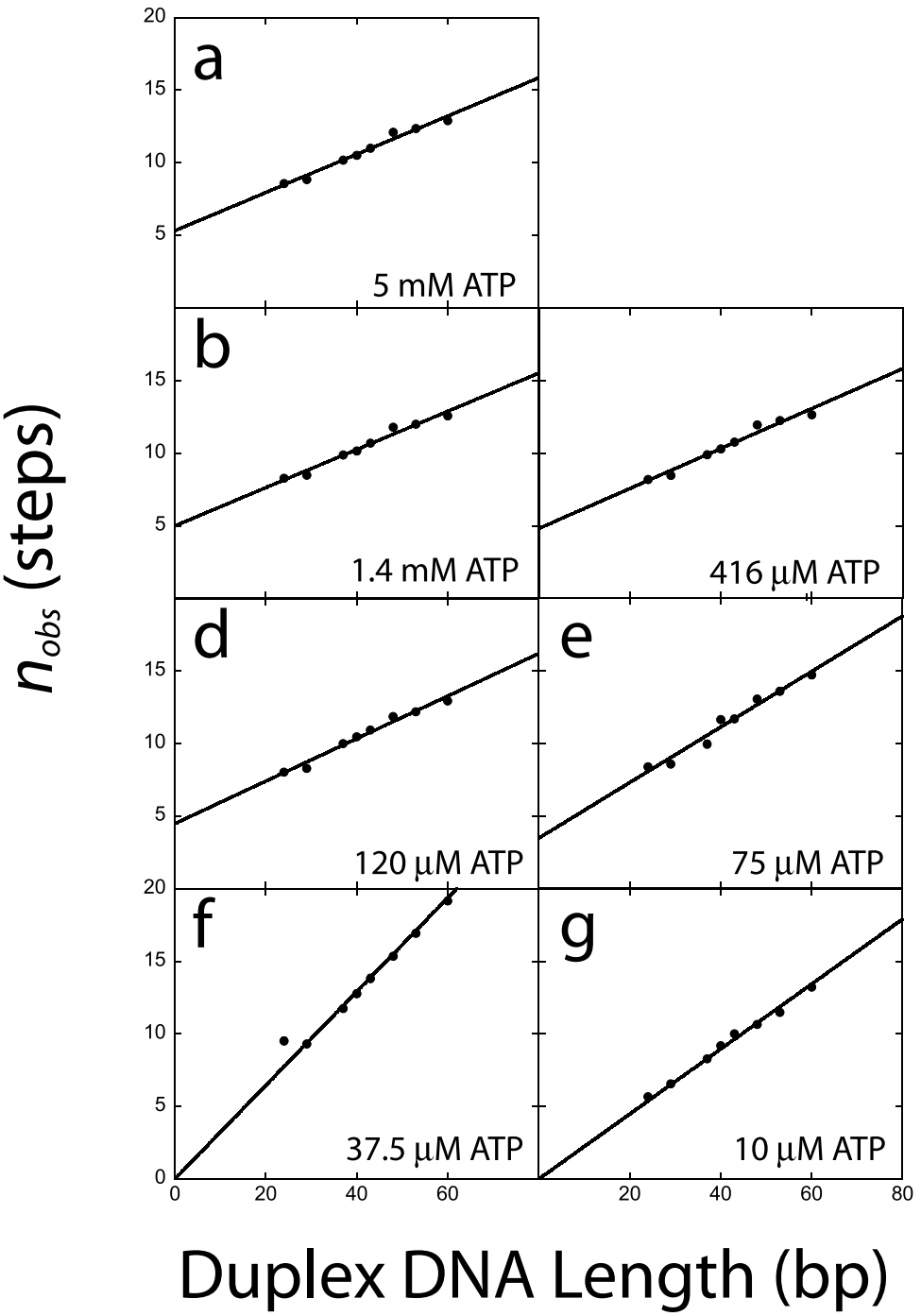

Figure 4. The dependence on duplex DNA length of the observed number of steps, n_{obs}, determined from analysis of the experimental RecBCD–DNA unwinding time-courses. Each set of time-courses at each [ATP] in Figure 3 was analyzed using Scheme 4 (equation (1)) by constraining the parameters k_U, and k_{NP} to be identical for each time-course, while A_1, x, and n were allowed to float for each time-course.

$$(R \bullet D)_{NP}$$
$$\downarrow k_{NP}$$
$$(R \bullet D)_L \xrightarrow{k_c} (R \bullet D)_L^1 \xrightarrow{k_c} \ldots (R \bullet D)_L^h \xrightarrow{k_u} I_{(L-m)} \xrightarrow{k_u} \ldots . I_{(L-im)} \ldots \xrightarrow{k_u} ssDNA$$

Scheme 5.

Quantitative analysis of the DNA unwinding time courses to determine the unwinding rate and kinetic step-size

The plots of n_{obs} *versus* L in Figure 4 all have similar slopes, with the exception of the data collected at 37.5 μM ATP (Figure 4f) which have a larger slope. As noted,[21,22] the slope of such plots should not be used directly to determine the kinetic step-size, since it can yield overestimates when additional kinetic steps are present that are not involved in DNA unwinding. Therefore, to determine the kinetic step-size at each ATP concentration, we re-analyzed the time-courses in Figure 3 using Scheme 5 (equation (3)), which includes additional steps with rate constants k_C that are not involved in the repeated unwinding cycles. Scheme 5 was used by us to analyze RecBCD-catalyzed DNA unwinding.[21,38] In our NLLS analysis using Scheme 5 (equation (3)), the parameters k_U, k_C, k_{NP}, h and m were constrained to be global parameters (i.e. the same for all time-courses), while A_1 and x were allowed to float for each time-course. The smooth lines in Figure 3 are simulations using Scheme 5 (equation (3)) and the best-fit NLLS parameters reported in Table 1.

Figure 5a indicates that the apparent unwinding rate constant, k_{Uapp}, decreases hyperbolically with decreasing [ATP]. An NLLS fit of these data to equation (5) yields $K_d = 176(\pm 30)$ μM, and a maximal unwinding rate constant at saturating [ATP], $k_{Umax} = 204(\pm 4)$ s^{-1}. Figure 5b shows the dependence on [ATP] of the macroscopic unwinding rate (bp s^{-1}), determined as the product of k_{Uapp} and the apparent step-size, m_{app}. A NLLS fit of $m_{app}k_{Uapp}$ *versus* [ATP] to equation (5) yields $K_d = 154(\pm 10)$ μM, with a maximal unwinding rate of $709(\pm 14)$ bp s^{-1}. Since the values of k_{Uapp} and m_{app} are >95% negatively correlated, the fit to equation (5) of the product, $m_{app}k_{Uapp}$, has lower uncertainties than the fit to k_{Uapp}. The dependence of the observed unwinding rate on [ATP] is in good agreement with previous reports for RecBCD.[16] Figure 5c shows that m_{app} for RecBCD-catalyzed DNA unwinding is independent of [ATP], with an average value of $3.7(\pm 0.4)$ bp step^{-1}.

The five sets of time-courses obtained at the highest ATP concentrations (Figure 3a–e) all fit best to Scheme 5 (equation (3)) with $h \sim 3$, where k_C ranges from 29 s^{-1} to 55 s^{-1} (Table 1), suggesting that three additional steps with rate constant k_C are needed to describe these time-courses. Within our uncertainties, both h and k_C appear to be independent of [ATP], although there is a suggestion of a slight decrease in k_C, with decreasing [ATP], as well as a slight decrease in the value of h (see Table 1). However, since the values of k_C and h are positively correlated, it is not likely that these slight trends are significant.

The decrease in k_{Uapp} with decreasing [ATP], coupled with the fact that k_C is independent of [ATP] explains the different behaviors of the plots

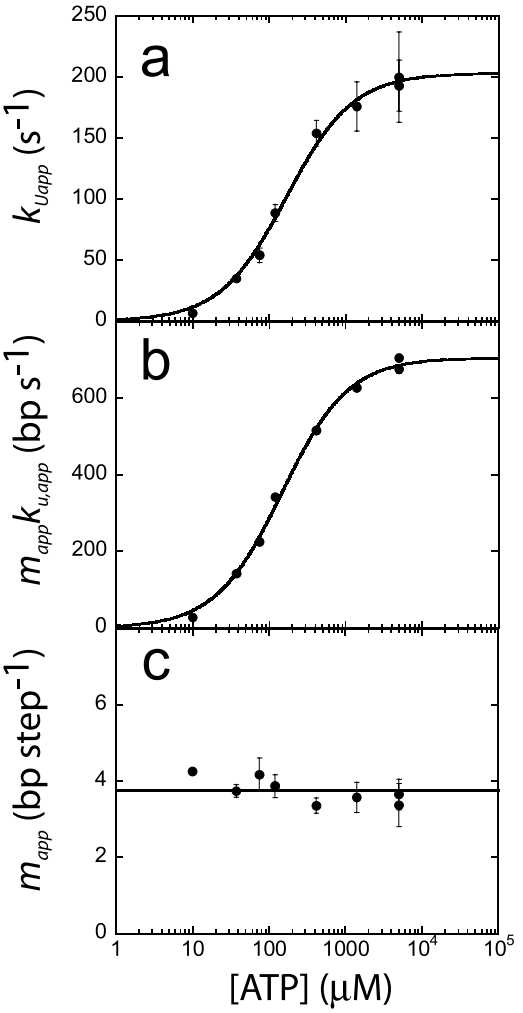

Figure 5. Dependence on [ATP] of the experimental kinetic parameters determined for RecBCD-catalyzed DNA unwinding. The kinetic parameters were determined from NLLS global fitting of each series of time-courses in Figure 3 to Scheme 5 (equation (3)). a, Dependence of k_{Uapp} (●) on [ATP] was fit to equation (5), yielding $(k_{Uapp})_{max} = 204(\pm 4)$ s^{-1}, and $K_d = 176(\pm 30)$ μM. b, The dependence of $m_{app}k_{Uapp}$ on [ATP] was fit to equation (5) yielding $(m_{app}k_{Uapp})_{max} = 709(\pm 14)$ bp s^{-1}, and $K_d = 154(\pm 10)$ μM. c, Dependence of the apparent kinetic step-size (m_{app}) on [ATP]. The average kinetic step size based on the seven determinations is $\langle m \rangle = 3.7(\pm 0.4)$ bp step^{-1} and indicated by the continuous line.

Table 1. Kinetic parameters determined from NLLS fitting of the data in Figure 3 to Scheme 5

Figure	[ATP]	k_U (s^{-1})	k_C (s^{-1})	k_{NP} (s^{-1})	m (bp $step^{-1}$)	h (steps)	mk_U (bp s^{-1})
3a	5 mM	193 ± 21	55 ± 3	6.2 ± 0.3	3.7 ± 0.4	3.5 ± 0.2	705 ± 9
3b	1.4 mM	176 ± 20	47 ± 2	5.4 ± 0.3	3.6 ± 0.4	3.1 ± 0.1	628 ± 7
3c	416 μM	154 ± 11	39 ± 1	4.3 ± 0.2	3.4 ± 0.2	2.8 ± 0.1	516 ± 5
3d	120 μM	89 ± 7	29 ± 1	3.8 ± 0.2	3.9 ± 0.3	2.9 ± 0.1	343 ± 3
3e	75 μM	54 ± 6	35 ± 8	6.0 ± 0.3	4.2 ± 0.4	3.0 ± 0.6	225 ± 4
3f	37.5 μM	35 ± 1	–	7.3 ± 0.1	3.11 ± 0.08	Zero steps	108 ± 1
	37.5 μM[a]	38 ± 1	38	7.2 ± 0.1	3.7 ± 0.1	Three steps	142 ± 2
3g	10 μM	6.35 ± 0.04	–	1.68 ± 0.01	4.25 ± 0.03	Zero steps	27.01 ± 0.03
Average			43 ± 10		3.7 ± 0.4	3.1 ± 0.2	

[a] This 37.5 μM data set is the same data as displayed in Figure 4f; however, the NLLS analysis was performed using equation (4) and constraining $h = 3$.

of n_{obs} *versus* L observed for the two lowest [ATP] (Figure 4f and g). At 37.5 μM ATP, the linear dependence of n_{obs} on L intersects the origin, but has a larger slope, 0.32 step bp^{-1} (~3.1 bp $step^{-1}$) than the plots at higher [ATP], which yield an average slope of 0.15(± 0.03) step bp^{-1} (7(± 1) bp $step^{-1}$). Whereas at still lower [ATP] (10 μM), the linear dependence still intersects the origin, but the slope increases to 0.23 step bp^{-1} (~4.4 bp $step^{-1}$). Based on Figure 5a, we see that at an [ATP] of ~37.5 μM, $k_{Uapp} = k_C$ (~38 s^{-1}). Therefore, at this [ATP], Scheme 5 collapses to Scheme 4, since one can no longer distinguish the steps with rate constant k_U from the steps with rate constant k_C. As a result, the plot of n_{obs} *versus* L at 37.5 μM ATP intersects the origin, yet the slope increases reflecting the fact that there appear to be more steps associated with DNA unwinding ($n + h$) than the true number of steps (n). As the [ATP] is lowered to 10 μM, where $k_C > k_{Uapp}$, the additional steps with rate constant k_C no longer limit the observed rate of unwinding and thus are not detectable. As a result, these additional steps affect neither the slope nor the intercept and thus the plot in Figure 4g intersects the origin and has an inverse slope of ~4.4 bp $step^{-1}$, which more accurately reflects the kinetic step-size determined for this set of data of (4.25 ± 0.03) bp $step^{-1}$ as determined from the global NLLS analysis (see Table 1).[22]

Effects of temperature on RecBCD-catalyzed DNA unwinding

As discussed above, if a single rate-limiting step is repeated for each DNA unwinding cycle at all temperatures, then the apparent kinetic step-size, m_{app}, should be independent of temperature. On the other hand, if two or more kinetic steps fortuitously have approximately the same rate-limiting value at a particular temperature, then m_{app} will be reduced.[22] To begin our discussion of potential effects of temperature, we first consider Scheme 6, which includes a reversible ATP-binding step followed by two additional steps with rate constants k_3 and k_4 per unwinding cycle (i.e. three repeating steps for every m bp unwound). Under conditions of excess [ATP], such that the ATP-binding rate will remain much faster than k_3 and k_4, then Scheme 6 will collapse to Scheme 7, which has only two repeating steps (k_3 and k_4) for every m bp unwound. If $k_3 = k_4$ at some temperature, then these two steps cannot be differentiated and the apparent step-size that is measured will be twofold lower than the actual value. However, if the two steps associated with these rate constants have different activation energies, E_a, then the apparent kinetic step-size will change with temperature. As such, DNA unwinding studies performed as a function of temperature might resolve the presence of two or more different kinetic steps that are repeated in the unwinding cycle.

To demonstrate this, we simulated a series of time-courses using Scheme 7 (equation (B2)), but then performed NLLS analyses on these simulated time courses using Scheme 1 (equation (A2)) to estimate k_{Uapp} and m_{app}. For these simulations we used the following parameters at 25 °C: $k_3 = 200\ s^{-1}$, (with $E_a = 20$ kcal mol^{-1}), $k_4 = 200\ s^{-1}$ (with $E_a = 0$), and $m = 4$ bp $step^{-1}$. A series of time-courses for $L = 24$, 30, 40, 48, and 60 bp were simulated for six temperatures ranging from 10 °C to 35 °C. The parameters determined from the NLLS analysis of these data using Scheme 1 are shown in Figure 6. Figure 6a and b show that the Arrhenius plots of k_{Uapp} and $m_{app}k_{Uapp}$, respectively, are non-linear. This is because k_4 is independent of temperature, whereas k_3 decreases with decreasing temperature, hence the rate limiting step in the cycle changes with temperature. At high temperatures $k_3 > k_4$ and thus k_4 is rate limiting, whereas at low temperatures $k_4 > k_3$ so that k_3 is rate limiting. At 25 °C, $k_3 = k_4$ and thus both steps are equally rate limiting.

$$HD_L + ATP \underset{k_2}{\overset{k_1}{\rightleftharpoons}} HD_L \cdot ATP \xrightarrow{k_3} HD_L^* \cdot ATP \xrightarrow{k_4} I_1 + ATP \underset{k_2}{\overset{k_1}{\rightleftharpoons}} I_1 \cdot ATP \xrightarrow{k_3} I_1^* \cdot ATP \xrightarrow{k_4} I_2 + ATP \ldots \xrightarrow{k_4} ssDNA$$

Scheme 6.

$$HD_L \xrightarrow{k_3} HD_L^* \xrightarrow{k_4} I_1 \xrightarrow{k_3} I_1^* \xrightarrow{k_4} I_2 \xrightarrow{k_3} I_3^* \ldots \xrightarrow{k_4} ssDNA$$

Scheme 7.

Figure 6c shows that the apparent kinetic step-size, m_{app}, estimated from the NLLS analysis, is lower than the input value of 4 bp at all temperatures, but displays curvature with a minimum at 25 °C. This results from the fact that neither k_3 nor k_4 becomes completely rate limiting at any of the temperatures examined. However, at 25 °C, where $k_3 = k_4$, a twofold underestimate of the kinetic step-size is obtained because both rate constants

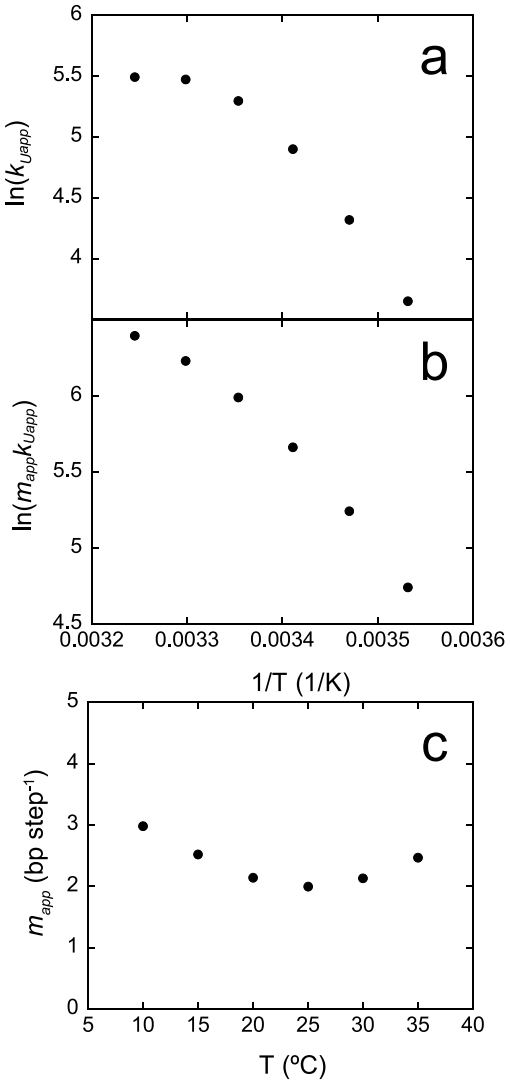

Figure 6. Dependence of simulated kinetic parameters on temperature. DNA unwinding time-courses were simulated using Scheme 7, but then underwent global NLLS analysis using Scheme 1 to obtain the indicated kinetic parameters. The simulations used the following parameters: $k_3 = 200\ s^{-1}$ with an activation energy of 20 kcal mol^{-1}; $k_4 = 200\ s^{-1}$, independent of temperature, $n = L/m$, $m = 4$ bp step^{-1}, and $L = 24$, 30, 40, 48, and 60 bp. a, Arrhenius plot for k_{Uapp}. b, Arrhenius plot for $m_{app}k_{Uapp}$. c, The effect of temperature on the apparent kinetic step-size, m_{app} determined from analysis of the simulated time-courses.

are identical and rate limiting, resulting in two repeating rate limiting steps per m bp unwound.

We examined the effect of temperature on RecBCD-catalyzed DNA unwinding using the single turnover fluorescence assay and the same eight DNA substrates described above (duplex lengths of 24–60 bp). Figure 7 shows the resulting DNA unwinding time-courses, monitoring Cy3 fluorescence, at 10, 15, 20, and 25 °C (5 mM ATP, 10 mM $MgCl_2$, 30 mM NaCl, (pH 7.0), 5% glycerol). These results show that the macroscopic rates of RecBCD–DNA unwinding increase with increasing temperature. NLLS analysis was performed on these data using Scheme 5 (equation (3)) and the continuous lines in Figure 7 are simulations based on Scheme 5 (equation (3)) and the best-fit kinetic parameters given in Table 2.

Figure 8a shows Arrhenius plots of the three apparent rate constants (k_{Uapp}, k_C, k_{NP}, and $m_{app}k_{Uapp}$) determined from analysis of the time courses in Figure 7. Each of these plots is linear within our uncertainties and linear least-squares analysis using equation (6) yields the apparent activation energies, E_a, reported in Table 3, with the apparent rate of unwinding having $E_a = 18.8(\pm 0.5)$ kcal mol^{-1}. Figure 8b shows a plot of the apparent kinetic step-size determined at each temperature. These values range from 3.9(±0.2) at 10 °C to 3.7(±0.4) at 25 °C, with an apparent optimum of 4.8(±0.3) at 15 °C, with the average of the four determinations, $\langle m \rangle = 4.2(\pm 0.5)$ bp step^{-1}. Figure 8c shows that the parameter h (the number of steps with rate constant k_C) is independent of temperature, with an average value of $\langle h \rangle = 3.3(\pm 0.2)$ steps.

Although there is a suggestion of a maximum in m_{app} at 15 °C, we do not believe that this is significant, and rather conclude that m_{app} is independent of temperature within our experimental uncertainty. In further support of this conclusion, we find that all schemes that we have considered that predict an effect of temperature on m_{app} always predict a minimum in m_{app} as a function of temperature (e.g. see Figure 6c), rather than a maximum. Therefore, we believe that the apparent maximum in the step-size is not likely to be significant. These results suggest that the same repeating kinetic step remains rate limiting in the DNA unwinding cycle at all of the temperatures investigated.

The temperature range we analyzed for these experiments (10–25 °C) is not extreme. In fact, we also performed DNA unwinding experiments at 30 °C and 37 °C (data not shown); however, the data obtained at these higher temperatures were too noisy to acquire a constrained fit from the NLLS analysis. As a result, we could not use these data to resolve individual values for the kinetic rate constants in Scheme 5. This seems primarily

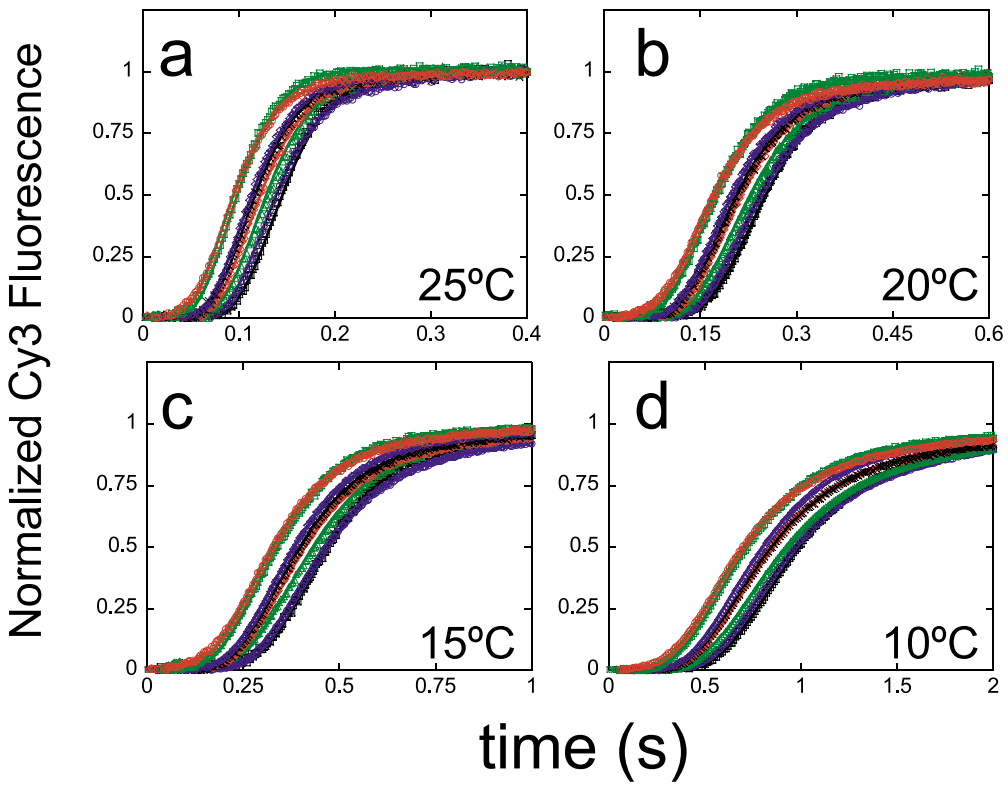

Figure 7. Effect of temperature on single turnover RecBCD-catalyzed DNA unwinding time courses. Stopped-flow kinetics experiments monitoring changes in Cy3 fluorescence of labeled DNA substrates experiments were performed by pre-incubating 200 nM RecBCD with 40 nM DNA substrate in buffer M at the indicated temperature. Reactions were initiated by rapidly mixing the RecBCD–DNA solution with a solution containing ATP (final [ATP] concentrations noted in each panel) and heparin (1.6 mg ml^{-1} final concentration) in buffer M. The Cy3 fluorophore was excited at $\lambda_{ex} = 515$ nm, and the Cy3 fluorescence was monitored at 570 nm using an interference filter. For each temperature (denoted for each panel), the Cy3 fluorescence time-courses are shown for duplex lengths: $L = 24$ bp (○), $L = 29$ bp (□), $L = 37$ bp (◇), $L = 40$ bp (×), $L = 43$ bp (+), $L = 48$ bp (△), $L = 53$ bp (○), and $L = 60$ bp (□). The smooth curves overlaying each time course are simulations using Scheme 5 (equation (3)) and the best-fit parameters given in Table 2.

due to the fact that the rate of RecBCD catalyzed DNA unwinding increases with increasing temperature,[16,17] which will also decrease the observed signal-to-noise. In fact, such a decrease in signal-to-noise can be seen by comparing the data at 25 °C and 10 °C in Figure 7a and d. The DNA unwinding rate we measure at 25 °C is ~700 bp s^{-1} and the reaction is complete within 200 ms for the $L = 60$ bp substrate. Using the activation energy of 18.8(±0.5) kcal mol^{-1} determined here, we predict an unwinding rate of ~1200(±10) bp s^{-1} and 2426(±21) bp s^{-1} at 30 °C and 37 °C, respectively. With these higher rates, the unwinding time-course would be complete in ~40–70 ms at 30 °C and ~20–40 ms at 37 °C for duplex lengths ranging from 24 bp to 60 bp, which would result in an even lower signal-to-noise at these higher temperatures. It is also possible that as the temperature is increased there could be increased breathing in the region near the nick in the DNA, resulting in a decreased signal-to-noise.

Roman & Kowalczykowski[16] and Eggleston *et al.*[24] have reported estimates of the activation energy for RecBCD catalyzed DNA unwinding in a range from 10 kcal mol^{-1} to 12 kcal mol^{-1}, which is smaller than our estimate of 18.8(±0.5) kcal mol^{-1}. Although we do not fully understand the basis for this difference, the different solution conditions used could contribute to this difference. It is also possible that the different assays used might be sensitive to different steps in the overall unwinding reaction. On the other hand, our

Table 2. Kinetic parameters determined from NLLS fitting of the data in Figure 7 to Scheme 5

Figure	Temperature (°C)	k_U (s^{-1})	k_C (s^{-1})	k_{NP} (s^{-1})	m (bp step^{-1})	h (steps)	mk_U (bp s^{-1})
7a	25	193 ± 21	55 ± 3	6.2 ± 0.3	3.7 ± 0.4	3.5 ± 0.2	705 ± 9
7b	20	97 ± 9	30 ± 1	4.4 ± 0.2	4.4 ± 0.4	3.3 ± 0.1	430 ± 5
7c	15	52 ± 4	15 ± 0.3	2.31 ± 0.03	4.8 ± 0.3	3.4 ± 0.05	252 ± 2
7d	10	33 ± 2	6.1 ± 0.1	1.02 ± 0.01	3.9 ± 0.2	3.02 ± 0.04	133 ± 1

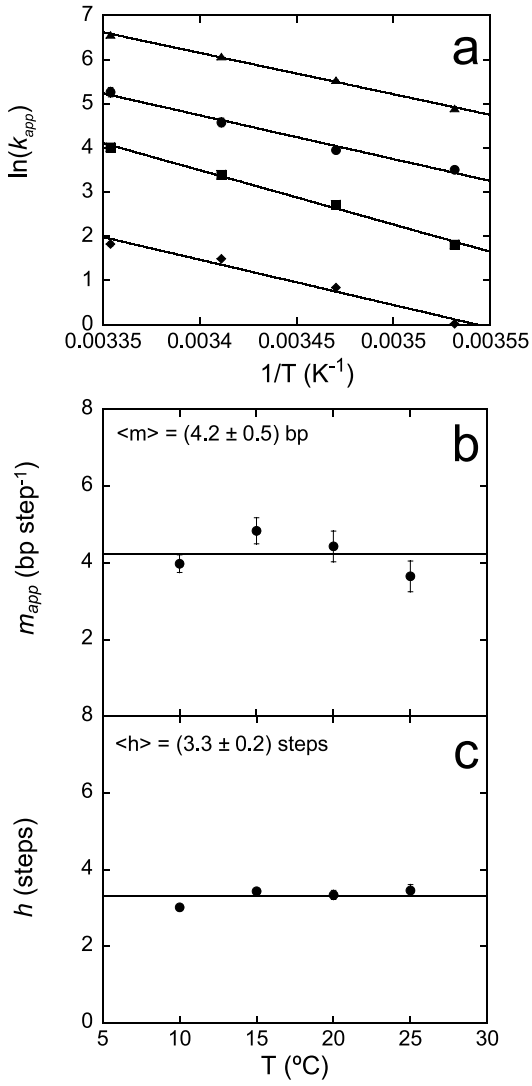

Figure 8. Dependence on temperature of the experimental kinetic parameters for RecBCD-catalyzed DNA unwinding. The experimental kinetic parameters were obtained from NLLS analysis of the time courses in Figure 7 using Scheme 5 (equation (3)). a, Arrhenius plots of mk_U (▲), k_U (●), k_C (■), and k_{NP} (◆). The continuous lines are simulations using equation (6) and the best-fit parameters determined from linear least-squares fitting reported in Table 3. b, Dependence of the apparent kinetic step-size, m_{app}, on temperature. The continuous line shows the average value of 4.2 bp step^{-1} determined for the four temperatures. c, Dependence on temperature of the number of steps, h, with rate constant kC. The continuous line shows the average value of 3.3 steps determined for the four temperatures.

Table 3. Activation energies determined from linear least-squares analysis of data in Figure 8a using equation (6)

Rate constant/Rate	E_a (kcal mol^{-1})
mk_U	18.8 ± 0.5
k_U	19 ± 1
k_C	25.5 ± 0.4
k_{NP}	23.2 ± 0.4

measurements were also made over a different temperature range (10–25 °C) than those in the previous studies (20–37 °C), hence it is also possible that the activation energy for unwinding is itself temperature dependent (decreasing with increasing temperature). However, although we cannot resolve the values of the individual kinetic rate constants needed to describe Scheme 5 from the unwinding experiments performed at 30 °C and 37 °C, we can predict the time-courses for unwinding at 30 °C and 37 °C based on Scheme 5 and the values of k_U, k_C, k_{NP} obtained from linear extrapolation of the Arrhenius plots made from the values obtained at temperatures below 25 °C, assuming a temperature-independent activation energy of 18.8(± 0.5) kcal mol^{-1}. We find that these predicted time-courses are consistent with the unwinding time-courses that we observe at 30 °C and 37 °C. Hence, our data do not suggest a significant decrease in activation energy at temperatures above 25 °C.

Discussion

Using the stopped-flow fluorescence assay developed described,[38] we have examined the effect of temperature and ATP concentration on the single turnover kinetics of RecBCD-catalyzed DNA unwinding. By examining the effect of duplex DNA length on these time-courses, one can obtain information about the intermediate steps that occur during DNA unwinding. In addition to obtaining the values of the rate constants for the rate-limiting steps in unwinding, one can also estimate an apparent kinetic step-size, m_{app}, for DNA unwinding. This kinetic step-size provides a measure of the average number of base-pairs unwound between two successive rate-limiting steps that are repeated during DNA unwinding. As such, this kinetic step-size would be equivalent to a mechanical step-size if only one rate-limiting step occurs for each mechanical step.[22] However, if two or more steps with rate constants that are similar in magnitude to the rate-limiting step occur within the repeated cycles, then the measured m_{app} will be smaller than the mechanical step-size.

In order to probe further the meaning of the kinetic step-size as measured in our single turnover DNA unwinding experiments, we examined whether it is affected by solution conditions, particularly [ATP] and temperature. The motivation for this study stems from the idea that if in fact two (or more) slow kinetic steps exist per DNA unwinding cycle that happen to have similar rate constants under one set of solution conditions, then one might be able to resolve these steps by examining unwinding under different solution conditions. The likelihood that the elementary rate constants for these multiple steps would possess the same dependencies on [ATP] and temperature would be expected to be small.

This is the first systematic examination of the effects of solution conditions on a kinetic step-size for a DNA helicase. Such a study is time-consuming, since each determination requires DNA unwinding time-courses to be obtained for several duplex DNA lengths and subjected to quantitative analysis under each set of solution conditions. Our studies were facilitated by two recent advances. The first is our development of a stopped-flow fluorescence assay for quantitative study of RecBCD catalyzed DNA unwinding,[38] which enabled us to acquire high precision time courses with a larger number of data points in a relatively short time and thus to vary the solution conditions more readily. The second advance is a novel method for NLLS analysis of kinetic time-courses described by n-step sequential mechanisms that enables one to float the kinetic step-size as a fitting parameter.[21,22] This has allowed us to access and explore the behavior of more complex mechanisms that would have been difficult to analyze quantitatively.[22]

Effect of [ATP] and temperature on the kinetics of RecBCD-catalyzed DNA unwinding

The DNA unwinding time-courses presented here are single turnover (single round) with respect to the DNA substrate, although multiple ATP turnovers can occur during a single turnover of DNA unwinding. Our previous studies of DNA unwinding maintained the [ATP] in large excess so that the rates of unwinding were not limited by the ATP-binding step.[21,25,26] However, when the [ATP] is lowered sufficiently, either the ATP-binding step or a step coupled to the ATP-binding step is expected to eventually become rate limiting. Hence, studies of the dependence of both the apparent unwinding rate constant and the apparent kinetic step-size on [ATP] can potentially yield information on the number of repeated rate-limiting steps that are monitored during each cycle of DNA unwinding. As discussed above, we define a cycle of DNA unwinding to include the set of kinetic steps (ATP binding, hydrolysis, ADP release, conformational changes, translocation, base-pair melting, etc.) that are repeated during the course of DNA unwinding, regardless of which step is rate limiting.

We find that, within our experimental uncertainties, the kinetic step-size for RecBCD-catalyzed DNA unwinding is independent of both temperature and [ATP], although the individual rate constants describing the mechanism vary considerably. This suggests that a single rate-limiting kinetic step occurs per repeated cycle of DNA unwinding and that this same kinetic step remains rate limiting under all conditions examined. The average value of the kinetic step-size is $4.2(\pm 0.5)$ bp step^{-1} at the four temperatures examined, and $3.7(\pm 0.4)$ bp step^{-1} at the seven ATP concentrations examined. As such, our best estimate of the DNA unwinding kinetic step-size is $3.9(\pm 0.5)$ bp step^{-1}, which is identical with the value determined using chemical quenched-flow techniques ($3.9(\pm 1.3)$ bp step^{-1}),[21] although with significantly improved precision.

The apparent unwinding rate constant, k_{Uapp}, exhibits a hyperbolic dependence on [ATP]. As suggested by the results of simulations presented in Figure 2, this indicates that the ATP-binding step is in rapid equilibrium with the subsequent step in the unwinding cycle (i.e. $k_2 \gg k_3$ in Scheme 2). This, along with the [ATP]-independent kinetic step-size, further suggests that the same repeated kinetic step remains rate-limiting at all [ATP] and that this step is coupled to ATP binding. The dependence of k_{Uapp} on [ATP] arises since the ATP-binding step is kinetically linked to the rate-limiting step that we are measuring (e.g. k_3 in Scheme 2 with $k_2 \gg k_3$). If there were a transition from monitoring a rate-limiting step of k_3 at high [ATP] to a rate-limiting step of ATP binding at low [ATP], then we would expect to observe a reduction in the step-size (possibly by as much as twofold) at some intermediate [ATP] where $k_1[\mathrm{ATP}] \approx k_3$, followed by a return to its higher value at still lower [ATP] as indicated in Figure 1b.

As in our previous studies, we have analyzed these kinetic data using a sequential n-step reaction scheme.[21,22,25] Furthermore, we have assumed that each repeating step is irreversible (with the exception of the ATP-binding step). The fact that the hyperbolic dependence of k_{Uapp} on [ATP] displays a zero y-intercept (see Figure 5a) further supports this assumption. If one has a two-step reaction, in which the first step is in rapid equilibrium, then the dependence on substrate concentration of the observed rate constant for the formation of final product, k_{obs}, will always be hyperbolic. However, if the second step is reversible, then k_{obs} will display a positive non-zero intercept corresponding to the reverse rate constant for this step, whereas if the second step is irreversible, then a zero intercept will be observed.[23] The dependence of k_{Uapp} on [ATP] suggests that the reverse rate for the second kinetic step (i.e. the step with rate constant k_3 in Scheme 2) can be considered zero on the time-scale of the next ATP-binding event.

Roman & Kowalczykowski[16] examined the dependence of RecBCD-catalyzed unwinding of linearized plasmid DNA by monitoring the intrinsic tryptophan fluorescence of SSB protein upon SSB binding to the ssDNA generated by RecBCD. Those studies reported a hyperbolic dependence of the observed unwinding rate on [ATP] with $K_{1/2} = 130(\pm 30)$ μM (25 °C, 25 mM Tris–acetate (pH 7.5), 1 mM magnesium acetate, 1 mM DTT). The value we report here of $154(\pm 10)$ μM for the dependence of the overall unwinding rate, $m_{\mathrm{app}}k_{\mathrm{Uapp}}$, on [ATP], is in good agreement with that study, although the solution conditions used are different.

Our studies also provide further support for the conclusion that the additional steps with rate constant k_{C} that are needed in the mechanism (see

Scheme 5) represent a set of conformational changes that precede the initiation of DNA unwinding. We had suggested that these steps are not involved in the DNA unwinding cycle based on three lines of evidence. The first is that the number of these steps is independent of duplex DNA length.[21,38] Second, our simulations predict that a positive non-zero intercept will be observed in a plot of n_{obs} *versus* L for a mechanism that includes additional steps not involved in repeating cycles of DNA unwinding, as is observed.[21,22] Finally, we also have direct evidence for multiple slow steps preceding the initiation of DNA unwinding.[38] The studies reported here indicate that the value of the rate constants for these steps, and their number, are also independent of [ATP], which also suggests that they are not involved in the DNA unwinding cycle.

What is the nature of the repeated rate-limiting step?

An important remaining question is whether the rate-limiting kinetic step that is measured in our single turnover DNA unwinding experiments reflects the actual DNA unwinding step, mechanical movement of the enzyme or some other process (e.g. protein conformational change, ADP release). Although we cannot answer this question based on only the experiments reported here, we can place constraints on the nature of this rate-limiting step. At a minimum, we can conclude that the repeated rate-limiting step is kinetically coupled to an ATP-binding step. That is, there cannot be any fast kinetic steps between the ATP-binding step and the repeated rate-limiting step. If there were, then a transition in the apparent step-size would be observed similar to that depicted in Figure 1(b) (see Appendix B, Scheme 6 with $k_3 \gg k_4$). However, as discussed above (see Theoretical Background), our experiments are not sensitive to the stoichiometry of ATP binding, thus the "ATP-binding step" observed here could involve multiple ATP binding events. Therefore, one can observe an apparent kinetic step-size that is independent of [ATP] even if there are multiple ATP-binding and hydrolysis events, where only one of them is coupled to a slow step. It is also possible that some ATP hydrolysis may not be tightly coupled to DNA unwinding. In fact, although both the RecB and RecD subunits can both bind and hydrolyze ATP, it is possible that only one ATP-binding site is tightly coupled to the DNA unwinding process.

A determination of whether ATP binding to one particular subunit is tightly coupled to DNA unwinding should be facilitated by studies of the RecBC helicase (RecBCD minus the RecD subunit). However, this will also require a full set of studies similar to those reported here to determine the kinetic step-size for RecBC and its dependence on [ATP]. On the other hand, we do observe that the lag phase and rate of unwinding of a single length duplex DNA are essentially the same for RecBC and RecBCD.[38] Although further study is required to determine if both RecBCD and RecBC enzymes use similar mechanisms, this suggests that the RecB subunit controls the rate of unwinding under these conditions and contains the ATPase site that is tightly coupled to DNA unwinding.

Among the possibilities for the rate-limiting step in DNA unwinding are the actual DNA unwinding step, such that m bp are melted in a single kinetic step, or the mechanical movement (translocation) of the enzyme. Another likely possibility is that the rate-limiting step reflects some conformational change in the enzyme that follows one or more rapid ATP binding/hydrolysis events. For example, a rate-limiting protein conformational change could follow several sequential, but rapid single base-pair unwinding steps, each coupled to ATP binding (see Scheme 3). However, if the rate-limiting conformational change occurs once for each mechanical step, then the kinetic step-size measured would still reflect the number of base-pair unwound per mechanical step.

The rate-limiting step is not a concerted "fraying" of multiple base-pairs of the DNA duplex

Our finding that the kinetic step-size for DNA unwinding is independent of temperature suggests that DNA unwinding proceeds by an active mechanism. An active mechanism is defined as one in which the helicase interacts directly with the duplex DNA and participates in the actual destabilization or melting of the m bp. This is in contrast to a passive mechanism in which a helicase simply translocates along the ssDNA in the direction of the duplex and traps ssDNA that is transiently formed through thermal fluctuations (i.e. thermal end fraying or "breathing") in the duplex DNA.[27] In a passive mechanism, if the rate-limiting step is the concerted fraying of m bp so that the helicase can move into the duplex with a step-size of m bp, one would expect the DNA unwinding step-size to decrease with decreasing temperature (i.e. with increasing stability of the DNA duplex). Although we have only spanned a range from 10 °C to 25 °C, our results provide no indication of a decreasing step-size with decreasing temperature. In fact, if anything, the data may suggest a slight increase with decreasing temperature.

The activation energy for DNA unwinding measured here ($E_a = 19(\pm 1)$ kcal mol^{-1}) also does not support a passive mechanism if all 4 bp were to fray in a concerted manner. If RecBCD were to unwind duplex DNA through such a passive mechanism, then our experiments suggest a lower limit of ~4 bp for the number of bp that must thermally fray before RecBCD can trap the frayed intermediate. Williams *et al.*[28] estimated an activation energy of ~41 kcal mol^{-1} for the melting of a 6 bp oligodeoxynucleotide. Using fluorescence

correlation spectroscopy, Bonnet *et al.*[29] estimated an activation energy of ~ 31 kcal mol^{-1} for the opening of a 5 bp hairpin DNA, independent of hairpin loop size. Since it is not known in these studies how many base-pairs must melt before the entire duplex melts, these activation energies represent lower limits for the activation energy for melting 4 bp at the end of a duplex. Irrespective of this, these activation energies are considerably larger than the ~ 19 kcal mol^{-1} that we measure for the activation energy for RecBCD-catalyzed unwinding of 4 bp of duplex DNA. As such, the data presented here are most consistent with an active mechanism for RecBCD-catalyzed DNA unwinding.

Materials and Methods

Buffers

Buffers were prepared with reagent grade chemicals using twice distilled H_2O, that was subsequently deionized with a Milli-Q purification system (Millipore Corp., Bedford, MA). RecBCD storage buffer is buffer C, which is 20 mM KPO_4 (pH 6.8), 0.1 mM β-ME, 0.1 mM EDTA, 10% glycerol. Buffer M is 20 mM Mops–KOH (pH 7.0), 30 mM NaCl, 10 mM $MgCl_2$, and 5% (v/v) glycerol. Buffers were titrated to pH 7.0 at each temperature.

Heparin (sodium salt) was purchased from Sigma (Sigma, St. Louis MO, Catalog No. H-3393) and was dialyzed extensively against water using 3500 molecular mass cut-off dialysis tubing. The concentration of the heparin stock solution was determined by titration with azure A,[30] which binds to the ionizable groups on the heparin polysaccharide.[31]

Proteins

E. coli RecBCD protein (fraction D) was purified as described[12,18,32] and was stored at −80 °C in buffer C. RecBCD concentration was determined spectrophotometrically using an extinction coefficient of $\varepsilon_{280} = 4.5 \times 10^5$ M^{-1} cm^{-1} for the hetero-trimer in buffer C;[21] all protein concentrations reported refer to the RecBCD hetero-trimer. RecBCD protein was dialyzed into final reaction conditions (buffer M) and stored at 4 °C for up to a week. RecBCD was not used for experiments after one week since an $\sim 5\%$ loss in activity was observed after this time.

Nucleic acids and DNA substrate design

The oligodeoxynucleotides used in this study were synthesized using an ABI model 391 (Applied Biosystems, Foster City, CA), and purified by electroelution of the DNA from denaturing polyacrylamide gels.[33] Fluorescently labeled DNA was subsequently purified by reverse phase HPLC using a C18 column (μ Bondpak, Waters) to separate the fluorescently labeled DNA from the non-labeled DNA, since these have identical mobility on a denaturing polyacrylamide gel. The concentrations of the DNA strands were determined by spectrophotometric analysis of the mixture of mononucleotides resulting after complete phosphodiesterase I digestion of the DNA in 100 mM Tris–HCl, 3 mM $MgCl_2$ (pH 9.2) at 25 °C as described.[34] For this analysis, the extinction coefficient for the free mononucleotides and the fluorophores at 260 nm are: 15,340 M^{-1} cm^{-1} for AMP; 7600 M^{-1} cm^{-1} for CMP; 12,160 M^{-1} cm^{-1} for GMP, 8700 M^{-1} cm^{-1} for TMP[35] and 5000 M^{-1} cm^{-1} for Cy3 and 10,000 M^{-1} cm^{-1} for Cy5 (Glenn Research). The nucleotide sequences used in these studies are given in Figure 1 of the accompanying paper,[38] with the exception of the bottom strand which is identical with that used and reported.[21] A stock solution of each DNA substrate was prepared by mixing equimolar concentrations of each of the three oligodeoxynucleotides in Buffer M, followed by heating to 90 °C for five minutes and slow cooling to 25 °C.

Fluorescence stopped flow kinetics

Stopped-flow experiments were performed as described.[38] All experiments were performed by first pre-incubating 200 nM RecBCD with 40 nM DNA substrate and 6 μM BSA in buffer M. The mixture of RecBCD and DNA was allowed to equilibrate on ice for five minutes before loading into the syringe where it was allowed to equilibrate for another five minutes at the designated temperature. The results were identical when the solution was either allowed to equilibrate on ice for 20 minutes before loading into the syringe or allowed to equilibrate for 20 minutes at the designated temperature. The RecBCD mixture was then rapidly mixed with a solution containing $2x$ mM ATP and heparin (3.25 mg ml^{-1}), in buffer M. This results in final reaction conditions of 100 nM RecBCD, 20 nM DNA, 3 μM BSA, x mM ATP, 1.6 mg ml^{-1} heparin trap, 20 mM Mops–KOH (pH 7.0), 10 mM $MgCl_2$, 30 mM NaCl, and 5% (v/v) glycerol at the designated temperature.

Analysis of kinetic data

All kinetic time-courses used in our analysis represent the average of 12–14 individual time-courses. For all time-courses that exhibit a lag phase, it was assumed that the constant fluorescence signal observed before enhancement is a measure of 100% duplex DNA for that experiment and therefore represents zero unwinding. As such, the first ten data points were averaged and this average was subtracted from all of the data points thereby forcing each trace to start from zero. Because the total fluorescence amplitude can vary for each duplex DNA sample, and for each experiment, the total fluorescence amplitude has not been analyzed here. However, the total fluorescence amplitude varies only within $\pm 9\%$ and we do not observe any systematic dependence on duplex DNA length. Although the raw data were analyzed, each trace and fit was normalized to unity for visualization purposes.

Single turnover DNA unwinding time-courses were initially analyzed using the "n-step" sequential mechanism given by Scheme 4.[21,22,25] In this Scheme, $(R{\cdot}D)_L$ represents pre-formed productive RecBCD–DNA complexes, which can rapidly initiate DNA unwinding upon addition of ATP. DNA unwinding proceeds in steps by unwinding an average of m bp per step with rate constant k_U to form the partially unwound DNA intermediates, I_{L-m}, I_{L-2m}, I_{L-3m}, etc. before eventually forming fully unwound ssDNA. In Scheme 4, L is the total number of base-pairs in the duplex DNA to be unwound, n is the number of steps required to fully

unwind the L bp, and m is the kinetic "step-size" (base-pairs unwound per step $= L/n$). The subscripts indicated for each intermediate, i, refer to the number of intact base-pairs remaining in each partially unwound duplex. Scheme 4 also incorporates the fact that some fraction of the DNA is initially bound to RecBCD in non-productive complexes, $(R{\cdot}D)_{NP}$, that must first slowly isomerize, with net rate constant k_{NP}, to form the productive $(R{\cdot}D)_L$ complexes before initiation of DNA unwinding can occur. RecBCD can, in principle, dissociate with rate constant k_d at each intermediate step along the unwinding pathway. However, we have not included any dissociation steps explicitly in our analysis, since RecBCD is known to be highly processive under these conditions.[15,21]

Global weighted NLLS fitting of the kinetic time courses for DNA unwinding to a particular kinetic scheme was performed by obtaining $f_{ss}(t)$ as the inverse Laplace transform of $F_{ss}(s)$ using numerical methods as described[21,22] (see also Appendix A). For example, NLLS fitting of the time-courses to Scheme 4 used equation (1):

$$f_{ss}(t) = A_1 \mathscr{L}^{-1} F_{ss}(s) = A_1 \mathscr{L}^{-1}\left(\frac{k_U^n (k_{NP} + sx)}{s(k_{NP} + s)(k_U + s)^n}\right) \quad (1)$$

where $f_{ss}(t)$ is the fraction of ssDNA formed as a function of time for Scheme 4, $F_{ss}(s)$ is the Laplace transform of $f_{ss}(t)$ for Scheme 4, $\mathscr{L}^{-1}$ is the inverse Laplace transform operator, s is the Laplace variable, A_1 is a fluorescence amplitude term accounting for the total fluorescence change observed for DNA unwinding, and x is the fraction of productively bound complexes given by equation (2):

$$x = \frac{(R{\cdot}D)_L}{(R{\cdot}D)_L + (R{\cdot}D)_{NP}} \quad (2)$$

where $(R{\cdot}D)_L$ is the concentration of RecBCD in the productive form, and $(R{\cdot}D)_{NP}$ is the concentration of RecBCD in the non-productive form. In brief, the NLLS fitting involved first obtaining the closed-form expression for $F_{ss}(s)$. The experimental time-courses were then fit to $f_{ss}(t)$, where $f_{ss}(t)$ was obtained by performing the inverse Laplace transform numerically as described.[21,22] Each time-point was weighted by the standard deviation of the point determined from the averaging of 12–14 time-courses. For global analysis of time-courses determined for a set of DNA substrates varying in duplex length using equation (1), the fluorescence amplitude (A_1), the fraction of productively bound complexes (x), and the number of steps (n), were allowed to have unique values for each duplex length (i.e. local parameters), whereas, k_U and k_{NP} were treated as global parameters, required to be the same for all duplex lengths.

NLLS analysis of DNA unwinding time-courses in each panel of Figures 3 and 7 was performed as described above using Scheme 5 (equation (3)):

$$f_{ss}(t) = A_1 \mathscr{L}^{-1} F_{ss}(s) = A_1 \mathscr{L}^{-1}\left(\frac{k_C^h k_U^{L/m} (k_{NP} + sx)}{s(k_C + s)^h (k_{NP} + s)(k_U + s)^{L/m}}\right) \quad (3)$$

where k_C is an additional slow step with h number of occurrences. When $h = 0$, Scheme 5 is equivalent to Scheme 4 and equation (3) reduces to equation (1). For global analysis of time-courses using equation (3), the amplitude (A_1) and the fraction of productively bound complexes (x) were allowed to have unique values for each duplex length, whereas, k_U, k_C, k_{NP}, h and m are all global parameters and are required to be the same for all duplex lengths.

We analyzed the experiments performed at 37.5 μM ATP (Figure 3f) using two Schemes. Our first attempt to analyze the time-courses at 37.5 μM ATP used Scheme 5 (equation (3)), which returned a value of $h = 0$ from the fitting. This is due to the fact that $k_U = k_C$ under these conditions. When $k_U = k_C$ equation (3) reduces to equation (4):[22]

$$f_{ss}(t) = A_1 \mathscr{L}^{-1} F_{ss}(s) = A_1 \mathscr{L}^{-1}\left(\frac{k_U^{L/m+h} (k_{NP} + sx)}{s(k_{NP} + s)(k_U + s)^{L/m+h}}\right) \quad (4)$$

where equation (4) is identical with equation (1) if the number of steps, n, is replaced with $L/m + h$. Therefore, these time-courses were also analyzed using equation (4), but constraining $h = 3$, which is equivalent to constraining $k_C = k_U$ in Scheme 5.

The ATP concentration dependence of the unwinding rate constant, k_{Uapp}, and the macroscopic unwinding rate, $m_{app}k_{Uapp}$, were fit to equation (5):

$$k_{app} = k_{max}\left(\frac{[ATP]_t}{K_d + [ATP]_t}\right) \quad (5)$$

where k_{max} can be either the maximal unwinding rate constant or the unwinding rate in bp s^{-1} and K_d is the equilibrium dissociation constant for ATP binding, and $[ATP]_t$ is the total [ATP].

The temperature dependencies of the kinetic parameters were analyzed using the Arrhenius equation (equation (6)):

$$\ln(k) = \ln(A) - \frac{E_a}{R}\frac{1}{T} \quad (6)$$

where E_a is the activation energy, and R is the ideal gas constant (1.987 cal mol^{-1}) and T is absolute temperature.

All NLLS fittings were performed using Conlin,[36] kindly provided by Dr Jeremy Williams. Fitting models were written in the programming language C and compiled using Microsoft's Visual C++ 6.0 compiler. The routine used in Conlin for the numerical inversion of the Laplace transform was purchased from Visual Numerics Incorporated (Houston, TX) contained within the IMSL C Numerical Libraries as described.[22] All uncertainties reported represent 68% confidence limits (±1 standard deviation). The parameter uncertainties obtained from NLLS fitting were determined by performing a 50 cycle Monte Carlo simulation[37] using the built-in routine available in Conlin.

Acknowledgements

We thank N. Maluf and C. Fischer for discussions throughout this research and C. Fisher and A. Niedziela-Majka for comments on the manuscript. We thank T. Ho for synthesis and purification of the DNA substrates. This research was supported in part by NIH grant (GM45948), and NIH training grant (5 T32 GM08492) (to A.L.L.).

References

1. Finch, P. W., Wilson, R. E., Brown, K., Hickson, I. D., Tomkinson, A. E. & Emmerson, P. T. (1986). Complete nucleotide sequence of the *Escherichia coli* recC gene and of the thyA-recC intergenic region. *Nucl. Acids Res.* **14**, 4437–4451.
2. Finch, P. W., Storey, A., Chapman, K. E., Brown, K., Hickson, I. D. & Emmerson, P. T. (1986). Complete nucleotide sequence of the *Escherichia coli recB* gene. *Nucl. Acids Res.* **14**, 8573–8582.
3. Finch, P. W., Storey, A., Brown, K., Hickson, I. D. & Emmerson, P. T. (1986). Complete nucleotide sequence of *recD*, the structural gene for the α subunit of Exonuclease V of *Escherichia coli*. *Nucl. Acids Res.* **14**, 8583–8594.
4. Smith, G. R. (1990). RecBCD enzyme. In *Nucleic Acids and Molecular Biology* (Eckstein, F. & Lilley, D. M. J., eds), pp. 78–98, Springer, Berlin.
5. Kowalczykowski, S. C., Dixon, D. A., Eggleston, A. K., Lauder, S. D. & Rehrauer, W. M. (1994). Biochemistry of homologous recombination in *Escherichia coli*. *Microbiol. Rev.* **58**, 401–465.
6. Gorbalenya, A. E. & Koonin, E. V. (1993). Helicases: amino acid sequence comparisons and structure–function relationships. *Curr. Opin. Struct. Biol.* **3**, 419–429.
7. Boehmer, P. E. & Emmerson, P. T. (1992). The RecB subunit of the *Escherichia coli* RecBCD enzyme couples ATP hydrolysis to DNA unwinding. *J. Biol. Chem.* **267**, 4981–4987.
8. Dillingham, M. S., Spies, M. & Kowalczykowski, S. C. (2003). RecBCD enzyme is a bipolar DNA helicase. *Nature*, **423**, 893–897.
9. Taylor, A. F. & Smith, G. R. (2003). RecBCD enzyme is a DNA helicase with fast and slow motors of opposite polarity. *Nature*, **423**, 889–893.
10. Goldmark, P. J. & Linn, S. (1972). Purification and properties of the recBC DNase of *Escherichia coli* K-12. *J. Biol. Chem.* **247**, 1849–1860.
11. Thaler, D. S. & Stahl, F. W. (1988). DNA double-chain breaks in recombination of phage λ and of yeast. *Annu. Rev. Genet.* **22**, 169–197.
12. Taylor, A. F. & Smith, G. R. (1985). Substrate specificity of the DNA unwinding activity of the recBC enzyme of *Escherichia coli*. *J. Mol. Biol.* **185**, 431–443.
13. Telander-Muskavitch, K. & Linn, S. (1982). A unified mechanism for the nuclease and unwinding activities of the recBC enzyme of *Escherichia coli*. *J. Biol. Chem.* **257**, 2641–2648.
14. Taylor, A. & Smith, G. R. (1980). Unwinding and rewinding of DNA by the RecBC enzyme. *Cell*, **22**, 447–457.
15. Roman, L. J., Eggleston, A. K. & Kowalczykowski, S. C. (1992). Processivity of the DNA helicase activity of *Escherichia coli* recBCD enzyme. *J. Biol. Chem.* **267**, 4207–4214.
16. Roman, L. J. & Kowalczykowski, S. C. (1989). Characterization of the helicase activity of the *Escherichia coli* RecBCD enzyme using a novel helicase assay. *Biochemistry*, **28**, 2863–2873.
17. Bianco, P. R., Brewer, L. R., Corzett, M., Balhorn, R., Yeh, Y., Kowalczykowski, S. C. & Baskin, R. J. (2001). Processive translocation and DNA unwinding by individual RecBCD enzyme molecules. *Nature*, **409**, 374–378.
18. Taylor, A. F. & Smith, G. R. (1995). Monomeric RecBCD enzyme binds and unwinds DNA. *J. Biol. Chem.* **270**, 24451–24458.
19. Ganesan, S. & Smith, G. R. (1993). Strand-specific binding to duplex DNA ends by the subunits of the *Escherichia coli* RecBCD enzyme. *J. Mol. Biol.* **229**, 67–78.
20. Farah, J. A. & Smith, G. R. (1997). The RecBCD enzyme initiation complex for DNA unwinding: enzyme positioning and DNA opening. *J. Mol. Biol.* **272**, 699–715.
21. Lucius, A. L., Vindigni, A., Gregorian, R., Ali, J. A., Taylor, A. F., Smith, G. R. & Lohman, T. M. (2002). DNA unwinding step-size of *E. coli* RecBCD helicase determined from single turnover chemical quenched-flow kinetic studies. *J. Mol. Biol.* **324**, 409–428.
22. Lucius, A. L., Maluf, N. K., Fischer, C. J. & Lohman, T. M. (2003). General methods for analysis of sequential "n-step" kinetic mechanisms: application to single turnover kinetics of helicase catalyzed DNA unwinding. *Biophys. J.* **85**, 2224–2239.
23. Johnson, K. A. (1992). Transient-state kinetic analysis of enzyme reaction pathways. In *The Enzymes*, pp. 1–61, Academic Press, Inc., New York.
24. Eggleston, A. K., Rahim, N. A. & Kowalczykowski, S. C. (1996). A helicase assay based on the displacement of fluorescent, nucleic acid-binding ligands. *Nucl. Acids Res.* **24**, 1179–1186.
25. Ali, J. A. & Lohman, T. M. (1997). Kinetic measurement of the step size of DNA unwinding by *Escherichia coli* UvrD helicase. *Science*, **275**, 377–380.
26. Jankowsky, E., Gross, C. H., Shuman, S. & Pyle, A. M. (2000). The DExH protein NPH-II is a processive and directional motor for unwinding RNA. *Nature*, **403**, 447–451.
27. Lohman, T. M. & Bjornson, K. P. (1996). Mechanisms of helicase-catalyzed DNA unwinding. *Annu. Rev. Biochem.* **65**, 169–214.
28. Williams, A. P., Longfellow, C. E., Freier, S. M., Kierzek, R. & Turner, D. H. (1989). Laser temperature-jump, spectroscopic, and thermodynamic study of salt effects on duplex formation by dGCATGC. *Biochemistry*, **28**, 4283–4291.
29. Bonnet, G., Krichevsky, O. & Libchaber, A. (1998). Kinetics of conformational fluctuations in DNA hairpin-loops. *Proc. Natl Acad. Sci. USA*, **95**, 8602–8606.
30. Jaques, L. B. (1977). Determination of heparin and related sulfated mucopolysaccharides. *Methods Biochem. Anal.* **24**, 203–312.
31. Mascotti, D. P. & Lohman, T. M. (1995). Thermodynamics of charged oligopeptide–heparin interactions. *Biochemistry*, **34**, 2908–2915.
32. Amundsen, S. K., Taylor, A. F., Chaudhury, A. M. & Smith, G. R. (1986). recD: the gene for an essential third subunit of exonuclease V. *Proc. Natl Acad. Sci. USA*, **83**, 5558–5562.
33. Wong, I., Chao, K. L., Bujalowski, W. & Lohman, T. M. (1992). DNA-induced dimerization of the *Escherichia coli* Rep helicase. allosteric effects of single-stranded and duplex DNA. *J. Biol. Chem.* **267**, 7596–7610.
34. Holbrook, J. A., Capp, M. W., Saecker, R. M. & Record, M. T., Jr (1999). Enthalpy and heat capacity changes for formation of an oligomeric DNA duplex: interpretation in terms of coupled processes of formation and association of single-stranded helices. *Biochemistry*, **38**, 8409–8422.
35. Gray, D. M., Hung, S. H. & Johnson, K. H. (1995). Absorption and circular dichroism spectroscopy of nucleic acid duplexes and triplexes. *Methods Enzymol.* **246**, 19–34.

36. Williams, D. J. & Hall, K. B. (2000). Monte Carlo applications to thermal and chemical denaturation experiments of nucleic acids and proteins. *Methods Enzymol.* **321**, 330–352.
37. Straume, M. & Johnson, M. L. (1992). Monte Carlo method for determining complete confidence probability distributions of estimated model parameters. *Methods Enzymol.* **210**, 117–129.
38. Lucius, A. L., Wong, C. J. & Lohman, T. M. (2004). Fluorescence stopped-flow studies of single turnover kinetics of *E. coli* RecBCD helicase-catalyzed DNA unwinding. *J. Mol. Biol.* **339**, this issue.

Appendix A
Inclusion of Reversible ATP Binding Steps into an *n*-step Sequential Mechanism

Here, we present the expressions needed to describe the effect of ATP concentration on the time-course of formation of completely unwound DNA molecules, $f_{ss}(t)$, for an n-step sequential mechanism. We have used the method of Laplace transforms as described[21,22] to obtain $f_{ss}(t)$. Using this approach, one first obtains the Laplace transform of $f_{ss}(t)$, referred to as $F_{ss}(s)$, where s is the Laplace variable. One can then obtain $f_{ss}(t)$ by taking the inverse Laplace transform of $F_{ss}(s)$, as indicated in equation (A1):

$$f_{ss}(t) = \mathscr{L}^{-1}F_{ss}(s) \tag{A1}$$

where $\mathscr{L}^{-1}$ is the inverse Laplace transform operator. In general, analytic solutions for $F_{ss}(s)$ can be obtained readily for even complex mechanisms, whereas one is not able to obtain a general analytic solution in the time domain (i.e. for $f_{ss}(t)$), except for relatively simple mechanisms. However, one can always obtain solutions for $f_{ss}(t)$ by performing the inverse Laplace transform operation on $F_{ss}(s)$ using numerical methods.[22] Therefore, for these discussions, we will limit our consideration to expressions for $F_{ss}(s)$ in the Laplace domain and obtain $f_{ss}(t)$ by numerical methods.

For reference purposes, we first consider the simplest n-step sequential mechanism shown in Scheme 1 in which a single rate-limiting step, with rate constant k_U, is repeated n times. The expression for $F_{ss}(s)$ for this Scheme was obtained[21,22] and is given in equation (A2):

$$F_{ss}(s) = \frac{k_{obs}^{n_{app}}}{s(k_{obs}+s)^{n_{app}}} \tag{A2}$$

where $k_{obs} = k_U$, and $n_{app} = n$, where L is the duplex length to be unwound and m is the kinetic step-size ($m = L/n$). As shown,[21,22] the inverse Laplace transform of equation (A2) can be easily found for this simple case (in fact, in analytic form) to yield $f_{ss}(t)$.

To include the effects of [ATP] we consider Scheme 2, which is the minimal mechanism that includes a reversible ATP-binding step associated with each unwinding cycle. In Scheme 2, k_1 is the bimolecular rate constant for ATP binding to the helicase-DNA complex, k_2 is the reverse rate constant for this step and k_3 is a step that immediately follows ATP binding. Use of the Laplace transform method to solve for $f_{ss}(t)$ for Scheme 2 requires that all of the steps be treated as first-order reactions. Thus, we consider only cases in which the [ATP] is sufficiently high ([ATP] $\gg$ [HD_0], or [I_i]) so that the ATP-binding step can be treated as a unimolecular step (i.e. k_1[ATP] can be considered constant). The expression for $F_{ss}(s)$, the Laplace transform of $f_{ss}(t)$ for Scheme 2, under pseudo first-order conditions is given by equation (A3):

$$F_{ss}(s) = \frac{(k_1[\mathrm{ATP}])^n k_3^n}{s(k_1[\mathrm{ATP}](k_3+s) + s(k_2+k_3+s))^n} \tag{A3}$$

If experiments are performed in a large excess of ATP such that k_1[ATP] $\gg k_3$, then Scheme 2 is equivalent to Scheme 1 and equation (A3) reduces to equation (A2), the Laplace transform for Scheme 1, but with $k_{obs} = k_3$. Therefore, at saturating [ATP] the time-course is sensitive to only the slowest repeating step per cycle, in this case, the step with rate constant k_3. Likewise, at limiting [ATP] (but where [ATP] $\gg$ [HD_0], or [I_i]), such that $k_3 \gg k_1$[ATP], the time-course is sensitive to only the ATP-binding step, and equation (A3) again reduces to equation (A2), but with $k_{obs} = k_1$[ATP]. In either of these two limits, the apparent number of steps, n_{app}, is equal to the number of repeating cycles, n, and thus the same kinetic step-size, $m_{app} = L/n$. We next consider the behavior at [ATP] between these two limiting cases.

Rapid equilibrium ATP-binding conditions ($k_2 \gg k_3$)

If ATP binding in Scheme 2 occurs as a rapid equilibrium (i.e. $k_2 \gg k_3$), then the expression for $F_{ss}(s)$ is given by equation (A4):

$$F_{ss}(s) = \frac{(K_1[\mathrm{ATP}])^n k_3^n}{s(K_1[\mathrm{ATP}]k_3 + (1+K_1[\mathrm{ATP}])s)^n} = \frac{(k_{obs})^n}{s(k_{obs}+s)^n} \tag{A4}$$

where $K_1 = k_1/k_2$ is the equilibrium constant for ATP binding and k_{obs} is given by equation (A5):

$$k_{obs} = \frac{k_3 K_1[\mathrm{ATP}]}{1+K_1[\mathrm{ATP}]} \tag{A5}$$

which has the same form as the observed rate constant for a simple two-step binding reaction.[23] Since equation (A4) has the same form as equation (A2), this predicts that when ATP binding occurs as a rapid equilibrium, only a single repeating rate-limiting step will occur at all [ATP] and therefore a constant step-size, $m_{app} = L/n$, will be observed for all [ATP]. Furthermore, the apparent rate constant, k_{obs}, will exhibit a hyperbolic dependence on [ATP] (see equation (A5)), as illustrated in Figure 2 of the main text.

ATP-binding step is not in rapid equilibrium ($k_2 \ll k_3$)

When ATP binding does not occur as a rapid equilibrium (i.e. if $k_2 \ll k_3$ in Scheme 2), then the apparent step-size, m_{app}, can change with [ATP], since the apparent number of rate-limiting steps, n_{app}, can change with [ATP]. As described above for Scheme 2, $n_{app} = n$ in the two limiting cases of $k_1[ATP] \ll k_3$, or $k_3 \ll k_1[ATP]$. However, when $k_3 = k_1[ATP]$, both k_3 and $k_1[ATP]$ will be rate limiting and thus the apparent number of steps, n_{app}, will be twofold larger than the actual number of steps, n. This is shown in equation (A6), which shows the form of equation (A3) in the limit as $k_1[ATP]$ approaches k_3, and k_2 approaches zero:

$$\lim_{k_2 \to 0} \lim_{k_1[ATP] \to k_3} \frac{(k_1[ATP])^n k_3^n}{s(k_1[ATP](k_3 + s) + s(k_2 + k_3 + s))^n} = \lim_{k_2 \to 0} \frac{k_3^{2n}}{s(k_2 s + (k_3 + s)^2)^n} = \frac{k_3^{2n}}{s(k_3 + s)^{2n}} \quad \text{(A6)}$$

Therefore, since the apparent step-size, $m_{app} = L/n_{app} = L/2n$, under conditions where $k_1[ATP] = k_3$, and $k_2 \ll k_3$, m_{app} will be underestimated by twofold (see Figure 1b of the main text). Hence, a change in n_{app}, m_{app} and k_{obs} will be observed as a function of [ATP] for Scheme 2 when the ATP-binding step does not occur as a rapid equilibrium. This behavior is illustrated in Figure 1 of the main text.

Appendix B
A Mechanism in Which Each Repeating Unwinding Cycle Consists of an ATP-binding Step Followed by Two Successive Rate-limiting Steps (Scheme 6)

Here, we consider Scheme 6 in which each repeating DNA unwinding cycle consists of an ATP-binding step followed by two successive steps, with rate constants k_3 and k_4. In this case, k_3 could denote ATP hydrolysis, while k_4 could denote product (ADP or P_i) release, DNA unwinding, or mechanical movement of the enzyme. The Laplace transform of $f_{ss}(t)$ for Scheme 6 under pseudo first-order conditions for ATP binding is given by equation (B1):

$$F_{ss}(s) = \frac{(k_1[ATP])^n k_3^n k_4^n}{s(k_1[ATP](k_3 + s) + s(k_2 + k_3 + s))^n (k_4 + s)^n} \quad \text{(B1)}$$

Again, if any one of the three repeated steps in the cycle, under a given set of conditions, is very slow relative to the other two steps, equation (B1) will reduce to equation (A2) with k_{obs} equal to the rate constant for the slowest step and $n_{app} = n$.

If the ATP-binding step in Scheme 6 is in rapid equilibrium (i.e. $k_2 \gg k_3$), and if $k_4 = k_3$, then a transition in the apparent step-size will be observed as a function of [ATP] for the following reasons. At high [ATP], the ATP-binding step is much faster than both k_3 and k_4. As such, Scheme 6 reduces to Scheme 7 and equation (B1) simplifies to equation (B2):

$$F_{ss}(s) \frac{k_3^n k_4^n}{s(k_3 + s)^n (k_4 + s)^n} \quad \text{(B2)}$$

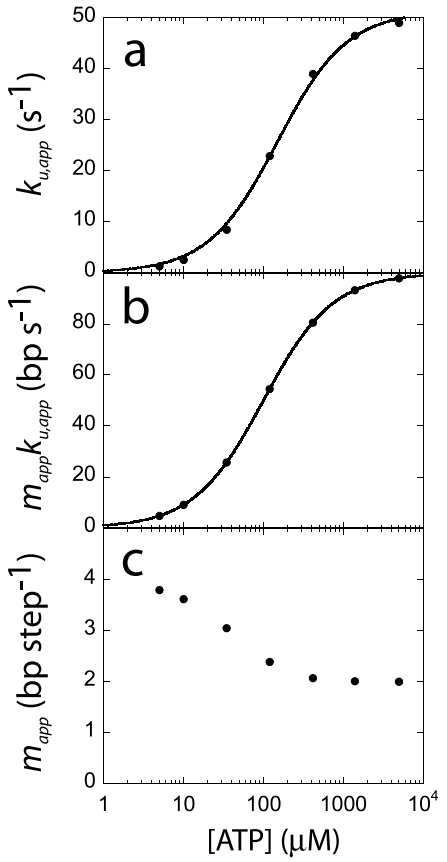

Figure B1. Dependence on ATP concentration of kinetic parameters obtained from analysis of simulated DNA unwinding time-courses generated using Scheme 6 (e.g. equation (B1)) when a rapid equilibrium applies to the ATP-binding step ($k_2 \gg k_3$). Time-courses were simulated using Scheme 6 and the following parameters: $k_1 = 1 \times 10^8\ M^{-1}\ s^{-1}$, $k_2 = 2 \times 10^4\ s^{-1}$ ($K_d = k_2/k_1 = 200\ \mu M$), $k_3 = 50\ s^{-1}$, $k_4 = 50\ s^{-1}$, $n = L/m$, $m = 4$ bp $step^{-1}$, for duplex lengths, $L = 24$, 30, 40, 48, and 60 bp. Global NLLS analysis of the simulated time-courses was then performed using Scheme 1 and the resulting best-fit kinetic parameters were determined. a, Hyperbolic dependence of k_{Uapp} on [ATP]. The continuous line is a simulation using equation (5) and the best NLLS parameters: $k_{Umax} = 51.3(\pm 0.8)\ s^{-1}$, and $K_d = 150(\pm 10)\ \mu M$. b, Hyperbolic dependence of $m_{app} k_{Uapp}$ on [ATP]. The continuous line is a simulation using equation (5) and the best NLLS parameters: $(m_{app} k_{Uapp})_{max} = 100$ bp s^{-1}, and $K_d = 100(\pm 0.1)\ \mu M$. c, The apparent kinetic step-size, m_{app}, exhibits a twofold transition from 2 bp $step^{-1}$ at excess ATP concentration to 4 bp $step^{-1}$ at limiting ATP concentration.

Therefore, at high [ATP], the time-courses are sensitive to two rate-limiting steps within each cycle of DNA unwinding. As such, the apparent step-size, $m_{app} = m/2$, since the apparent number of steps will be twofold larger than the number of unwinding cycles, n (see Figure B1c at excess ATP). However, since the ATP-binding step is kinetically linked to the step with rate constant k_3, as the [ATP] is decreased, the step with rate constant k_4 will become fast, relative to the other steps, and thus only a single rate-limiting step, coupled to k_3, will occur per unwinding cycle, resulting in an increase in m_{app} as indicated in Figure B1c. (N.B., since the ATP-binding step is in rapid equilibrium, the ATP-binding step never becomes rate-limiting as long as [ATP] remains in excess over the enzyme concentration).

Figure 5c suggests that there may be a slight increase in the observed kinetic step-size for RecBCD-catalyzed DNA unwinding as the [ATP] is decreased, although we believe these values are the same within our experimental uncertainty. However, if this trend is real, Scheme 6 could provide a possible explanation. To demonstrate this, time-courses were simulated using Scheme 6 (equation (B1)) with $k_1 = 1 \times 10^8\ M^{-1}\ s^{-1}$, $k_2 = 2 \times 10^4\ s^{-1}$, $k_3 = 50\ s^{-1}$, $k_4 = 50\ s^{-1}$, $n = L/m$, $m = 4$ bp step^{-1}, for $L = 24$, 30, 40, 48, and 60 bp and [ATP] ranging from 10 μM to 5 mM. Therefore, the ATP-binding step is in rapid equilibrium ($k_2 \gg k_3$) and $k_4 = k_3$. These time-courses were then fit to Scheme 1 to obtain the values of k_{Uapp} and m_{app} shown in Figure B1.

A NLLS analysis was performed on these data using equation (5) which results in best-fit parameters of a maximum $k_{Uapp,max} = 51.3(\pm 0.8)\ s^{-1}$, and $K_d = 150(\pm 10)$ μM. The continuous line in Figure B1a is a simulation using equation (5) and these parameters. The K_d used for generating the simulated time-courses was 200 μM, whereas the value determined from the NLLS analysis of Figure B1a yields an underestimate at 150(± 10) μM. Figure B1b is a plot of $m_{app}k_{Uapp}$ *versus* ATP concentration, an NLLS analysis was performed on these data using equation (5), which yields best-fit parameters of a maximum $(m_{app}k_{Uapp})_{max} = 99.98(\pm 0.01)\ s^{-1}$, and $K_d = 99.92(\pm 0.06)$ μM. As with the NLLS analysis of the hyperbolic dependence of k_{Uapp} on [ATP], the hyperbolic dependence of $m_{app}k_{Uapp}$ on [ATP] also yields an underestimate of the true K_d for these simulations.

The kinetic parameters used to simulate the time-courses for Scheme 6 result in a twofold decrease in m_{app} with increasing [ATP], as shown in Figure B1c. This is a much larger effect than suggested by the data shown in Figure 5c. This smaller effect of [ATP] can be described by Scheme 6 if $k_4 > k_3$ but not large enough so that k_3 becomes completely rate limiting. To illustrate this, we performed simulations as above, but with k_4 being five, ten, and 20-fold faster than k_3 at excess [ATP]. The changes in the apparent kinetic step-size determined from analysis of these time-courses using Scheme 1 are shown in Figure B2 and range from twofold to zerofold, depending on the relative rates of k_3 and k_4 in Scheme 6. Therefore, the slight change in m_{app} suggested by the data in Figure 5c could be obtained if Scheme 6 applies with $k_4 = 20k_3$. In this case, the time courses obtained at the lower [ATP] would provide the best estimate of m_{app}. However, this effect is clearly small, since the step-size determined at the lowest [ATP] (10 μM) is 4.25(± 0.03) bp step^{-1}, which is the same as the average step-size 3.9(± 0.5) bp step^{-1}) estimated from all determinations reported here.

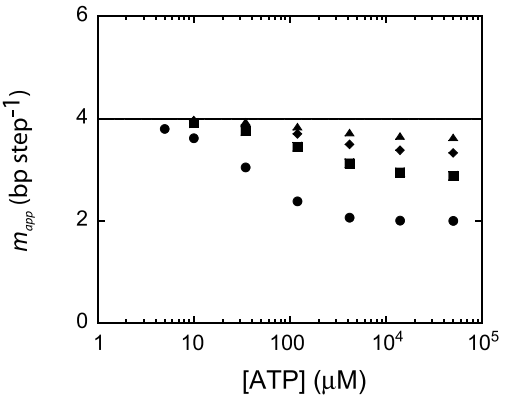

Figure B2. Dependence on ATP concentration of the apparent kinetic step-size obtained from analysis of simulated DNA unwinding time-courses generated using Scheme 6. For these simulations the ATP-binding step is in rapid equilibrium ($k_2 \gg k_3$) and $k_4 \geq k_3$. Time-courses were simulated using Scheme 6 and the following parameters: $k_1 = 1 \times 10^8\ M^{-1}\ s^{-1}$, $k_2 = 2 \times 10^4\ s^{-1}$, $k_3 = 50\ s^{-1}$, $n = L/m$, $m = 4$ bp step^{-1}, for $L = 24$, 30, 40, 48, and 60 bp, and: (●) $k_4 = k_3$; (■) $k_4 = 5k_3$; (◆) $k_4 = 10k_3$; (▲) $k_4 = 20k_3$. The horizontal line is drawn at $m_{app} = 4$ bp step^{-1}.

Demonstration that there can be no fast steps between ATP binding and the rate-limiting step being monitored at all [ATP] for RecBCD-catalyzed DNA unwinding

Scheme 2 is the simplest mechanism that can describe the RecBCD-catalyzed DNA unwinding time-course, based on our observations of a hyperbolic dependence of k_{obs} on [ATP] and a kinetic step-size that is independent of [ATP]. Based on these observations one can also conclude that the ATP-binding step occurs as a rapid equilibrium and that the same kinetic step, with rate constant k_3, remains rate limiting at all [ATP]. However, one can also conclude that no fast kinetic steps can occur between the ATP-binding step and the rate-limiting step with rate constant k_3. This can be demonstrated using Scheme 6, which has an additional step with rate constant k_4 in each cycle. If we constrain Scheme 6 such that $k_2 \gg k_3$ (ATP-binding step is in rapid equilibrium) and $k_3 \gg k_4$, this describes the situation in which a fast kinetic

step, k_3, exists between the ATP-binding step and the rate-limiting step, k_4.

Time-courses were simulated using Scheme 6 with the same values of k_1, k_2 and k_4 and m as used above ($k_1 = 1 \times 10^8\ M^{-1}\ s^{-1}$, $k_2 = 2 \times 10^4\ s^{-1}$, $k_4 = 50\ s^{-1}$, $m = 4$ bp step^{-1}), but with $k_3 = 1000\ s^{-1}$, so that $k_3 \gg k_4$, for $L = 24$, 30, 40, 48, and 60 bp and [ATP] ranging from 10 μM to 5 mM). These simulated time-courses were then fit to Scheme 1 to obtain values of k_{Uapp} and the apparent kinetic step-size, m_{app}. The resulting dependence of m_{app} on [ATP] is qualitatively similar to that shown in Figure 1b in that m_{app} goes through a minimum at intermediate [ATP]. This occurs for the following reasons. When ATP is in large excess, only the step with rate constant k_4 is rate limiting, so that only a single rate-limiting step occurs within the cycle, hence $m_{app} = 4$. However, in Scheme 6, the effect of [ATP] is coupled only to the step with rate constant k_3, since $k_3 \gg k_4$. As such, and since $k_2 \gg k_3$, the ATP-binding step and the step with rate constant k_3 can be considered as a single step with rate constant $k_{obs} = (k_3 K_1[ATP]/(1 + K_1[ATP]))$ (see equation (A5) in Appendix A). Therefore, as the [ATP] is lowered, k_{obs} will eventually decrease to a value where it is comparable in magnitude to k_4. In this range of [ATP] there will be two comparably slow steps in each unwinding cycle and thus a transition in m_{app} will be observed. Since we do not observe this behavior for RecBCD-catalyzed DNA unwinding (see Figure 5c), we conclude there are no fast steps between the ATP-binding step and the rate-limiting step in the unwinding cycle.

Edited by D. E. Draper

(Received 15 December 2003; received in revised form 1 April 2004; accepted 1 April 2004)